Neurobiology of Disease

tPA Deficiency Underlies Neurovascular Coupling Dysfunction by Amyloid-β

Laibaik Park, Joan Zhou, Kenzo Koizumi, Gang Wang, Antoine Anfray, Sung Ji Ahn, James Seo, Ping Zhou, Lingzhi Zhao, Steven Paul, Josef Anrather, and Costantino Iadecola

Feil Family Brain and Mind Research Institute, Weill Cornell Medicine, New York, New York 10065

The amyloid-β (Aβ) peptide, a key pathogenic factor in Alzheimer's disease, attenuates the increase in cerebral blood flow (CBF) evoked by neural activity (functional hyperemia), a vital homeostatic response in which NMDA receptors (NMDARs) play a role through nitric oxide, and the CBF increase produced by endothelial factors. Tissue plasminogen activator (tPA), which is reduced in Alzheimer's disease and in mouse models of Aβ accumulation, is required for the full expression of the NMDAR-dependent component of functional hyperemia. Therefore, we investigated whether tPA is involved in the neurovascular dysfunction of Aβ. tPA activity was reduced, and the tPA inhibitor plasminogen inhibitor-1 (PAI-1) was increased in male mice expressing the Swedish mutation of the amyloid precursor protein (tg2576). Counteracting the tPA reduction with exogenous tPA or with pharmacological inhibition or genetic deletion of PAI-1 completely reversed the attenuation of the CBF increase evoked by whisker stimulation but did not ameliorate the response to the endothelium-dependent vasodilator acetylcholine. The tPA deficit attenuated functional hyperemia by suppressing NMDAR-dependent nitric oxide production during neural activity. Pharmacological inhibition of PAI-1 increased tPA activity, prevented neurovascular uncoupling, and ameliorated cognition in 11- to 12-month-old tg2576 mice, effects associated with a reduction of cerebral amyloid angiopathy but not amyloid plaques. The data unveil a selective role of the tPA in the suppression of functional hyperemia induced by Aβ and in the mechanisms of cerebral amyloid angiopathy, and support the possibility that modulation of the PAI–1-tPA pathway may be beneficial in diseases associated with amyloid accumulation.

Significance Statement

Amyloid-β (Aβ) peptides have profound neurovascular effects that may contribute to cognitive impairment in Alzheimer's disease. We found that Aβ attenuates the increases in blood flow evoked by neural activation through a reduction in tissue plasminogen activator (tPA) caused by upregulation of its endogenous inhibitor plasminogen inhibitor-1 (PAI-1). tPA deficiency prevents NMDA receptors from triggering nitric oxide production, thereby attenuating the flow increase evoked by neural activity. PAI-1 inhibition restores tPA activity, rescues neurovascular coupling, reduces amyloid deposition around blood vessels, and improves cognition in a mouse model of Aβ accumulation. The findings demonstrate a previously unappreciated role of tPA in Aβ-related neurovascular dysfunction and in vascular amyloid deposition. Restoration of tPA activity could be of therapeutic value in diseases associated with amyloid accumulation.

Introduction

Cerebral blood vessels are endowed with sophisticated regulatory mechanisms that ensure an adequate blood flow delivery to the brain at all times. Of vital importance is functional hyperemia, a mechanism that couples the delivery of cerebral blood flow (CBF) to the energy requirements of local brain cells (Iadecola, 2017). Alterations in neurovascular coupling may compromise the energy balance of the brain and have been linked to brain dysfunction and cognitive impairment (Iadecola, 2013; Sweeney et al., 2018).

Alzheimer's disease (AD) is characterized neuropathologically by amyloid-β (Aβ) deposits in the brain parenchyma (amyloid plaques) and blood vessels [cerebral amyloid angiopathy (CAA)], and by intraneuronal accumulation of hyperphosphorylated tau

Received May 11, 2020; revised July 29, 2020; accepted Aug. 28, 2020.

Author contributions: L.P. and C.I. designed research; L.P., J.Z., K.K., G.W., A.A., S.J.A., J.S., and L.Z. performed research; L.P., J.Z., K.K., G.W., A.A., S.J.A., J.S., P.Z., L.Z., S.P., J.A., and C.I. analyzed data; L.P. and C.I. wrote the paper.

C.I. serves on the advisory board of Broadview Ventures. The authors declare no other competing financial interests.

This study is supported by National Institute of Neurological Disorders and Stroke and National Institute on Aging Grants R01-NS-097805 (to L.P.); and R01-NS-100447 and R01-NS37853 (to C.I.). Additional support was supplied by the Feil Family Foundation.

Correspondence should be addressed to Laibaik Park at lap2003@med.cornell.edu.

https://doi.org/10.1523/JNEUROSCI.1140-20.2020

(Long and Holtzman, 2019). Aβ, a 38–42 aa peptide cleaved from amyloid precursor protein (APP), is a major culprit in AD and exerts detrimental cerebrovascular effects (Cortes-Canteli and Iadecola, 2020). AD is associated with alterations in CBF (Iturria-Medina et al., 2016) and impaired neurovascular coupling early in the course of the disease (Iturria-Medina et al., 2016; Iadecola, 2017). Studies in mice overexpressing mutated APP indicate that Aβ peptides impair neurovascular coupling as well as the regulation of CBF by cerebral endothelial cells (Iadecola et al., 1999; Tong et al., 2012; Nortley et al., 2019). Considering the potential impact of CBF dysregulation on AD pathogenesis (Iturria-Medina et al., 2016; Long and Holtzman, 2019; Cortes-Canteli and Iadecola, 2020), elucidating the mechanisms by which Aβ alters neurovascular coupling could lead to new approaches to mitigate the disease.

Tissue plasminogen activator (tPA) is a serine protease best known for its role in intravascular fibrinolysis, glutamate neurotransmission, and synaptic plasticity (Baranes et al., 1998; Benchenane et al., 2004; Samson and Medcalf, 2006; Diaz et al., 2019). In addition, tPA is required for the full expression of functional hyperemia (Park et al., 2008a; Iadecola, 2017; Anfray et al., 2020). Mice lacking tPA have a marked attenuation in the increase in CBF induced by neural activity, resulting from reduced production of nitric oxide (NO) during the activation of NMDA receptors (NMDARs), one of the drivers of function hyperemia (Park et al., 2008a; Iadecola, 2017).

Interestingly, tPA is reduced in AD brains and in mice overexpressing APP, because of increased activity of the endogenous tPA inhibitor plasminogen activator inhibitor-1 (PAI-1; Melchor et al., 2003; Cacquevel et al., 2007; Jacobsen et al., 2008; Cortes-Canteli and Iadecola, 2020). These findings raise the possibility that reduced tPA activity may contribute to the harmful neurovascular effects of Aβ. Therefore, we examined the role of tPA in the neurovascular dysfunction and cognitive deficits induced by Aβ. We found that tPA activity is reduced in mice expressing mutated APP (tg2576) and that such reduction is responsible for the attenuation of functional hyperemia through the suppression of NMDAR-induced NO production. The tPA deficit does not contribute to the endothelial dysfunction, attesting to the selectivity of the effect on neurovascular coupling. Sustained rescue of tPA activity by PAI-1 inhibition restores neurovascular coupling, reduces CAA, and improves cognition in aged tg2576 mice without affecting amyloid plaques. The data unveil a new mechanism for the neurovascular coupling dysfunction induced by Aβ and suggest that the PAI-1–tPA pathways may be a putative target to counteract the harmful neurovascular effects of Aβ and the cognitive impact of CAA.

Materials and Methods

Mice. All procedures were approved by the Institutional Animal Care and Use Committee of Weill Cornell Medicine and performed according to the ARRIVE guidelines (Percie du Sert et al., 2020), and, whenever feasible, experiments were performed in a blinded fashion. The laser-Doppler flowmetry experiments, performed in a blinded fashion, were independently reproduced by two operators (L.P. and A.A.). We used 3- to 12-month-old transgenic mice overexpressing the Swedish mutation of the APP (tg2576; Hsiao et al., 1996). These ages were selected because at 3 months of age there is no amyloid deposition or cognitive deficit, whereas at 12 months there are abundant plaques, CAA, and cognitive deficits. We also used 3-month-old mice lacking tPA (Carmeliet et al., 1994) or PAI-1 (Carmeliet et al., 1993). In all studies, age-matched wild-type (WT) littermates as controls. All mice were males and congenic on a C57BL6 background. We did not use female mice because of the effect of the estrous cycle on cerebrovascular regulation, which would introduce variability and confound the interpretation of the results (Girouard et al., 2008; Capone et al., 2009).

General surgical procedures. Mice were anesthetized with isoflurane (maintenance, 2%), intubated, and artificially ventilated (SAR-830 small animal ventilator, CWE; Park et al., 2008b, 2017; Uekawa et al., 2016). The femoral vessels were cannulated for recording of arterial pressure, and blood sample collection (Iadecola et al., 1999; Uekawa et al., 2016; Park et al., 2017). Rectal temperature was maintained at 37°C. After surgery, isoflurane was gradually discontinued and anesthesia was maintained with urethane (750 mg/kg, i.p.) and α-chloralose (50 mg/kg, i.p.; Park et al., 2008b, 2017; Uekawa et al., 2016).

Recording of CBF and vascular reactivity. As in previous studies by us and others (Park et al., 2008a, 2014, 2020; Tong et al., 2012), we used the cerebral cortex to investigate the role of tPA in the neurovascular dysfunction of Aβ. We studied the neocortex because (1) it is easily accessible for experimental manipulations and dynamic measurement of CBF and (2) neurovascular uncoupling is also observed in the cerebral cortex of patients with AD (Mentis et al., 1998; Smith et al., 2008). A 2×2 mm opening was drilled in the parietal bone overlying the somatosensory cortex, the dura was removed, and the site was superfused with a modified Ringer's solution, at 37°C and pH 7.3–7.4 (Iadecola et al., 1999). Relative CBF was continuously monitored at the site of superfusion with a laser-Doppler probe (Vasamedic) positioned stereotaxically on the neocortical surface and connected to a computerized data acquisition system. CBF values were expressed as a percentage increase relative to the resting levels before and after treatment in the same mouse. Resting CBF is reported as laser-Doppler perfusion units (LDU). Arterial blood pressure and blood gases were monitored and controlled. CBF recordings were started after arterial pressure (mean arterial pressure, 78–85 mmHg) and blood gases [partial pressure of oxygen (pO_2), 120–140 mmHg; pO_2, 33–40 mmHg; pH 7.3–7.4) were in a steady state (Iadecola et al., 1999; Uekawa et al., 2016; Park et al., 2017). For functional hyperemia, the whiskers were mechanically stimulated for 60 s and the associated increase in CBF recorded over the somatosensory cortex. To investigate the effect of the low-density lipoprotein receptor-related protein 1 (LRP1) inhibitor receptor-associated protein (RAP; Shibata et al., 2000; Deane et al., 2004) on functional hyperemia, this agent (200 nM; Molecular Innovations) was superfused over the somatosensory cortex, and its effect was tested 30–40 min later. To test endothelium-dependent and endothelium-independent responses, acetylcholine (ACh; 10 μM; Sigma-Aldrich) and adenosine (400 μM; Sigma-Aldrich), respectively, were superfused and the resulting changes in CBF monitored (Uekawa et al., 2016; Park et al., 2017). In some mice, NMDA (10–40 μM; Sigma-Aldrich), AMPA (2–20 μM; Sigma-Aldrich), or kainate (2–20 μM; Sigma-Aldrich) was topically superfused on the cranial window. These concentrations were previously established not to induce cortical spreading depression, which also causes CBF increases (Park et al., 2008a). In other experiments, CBF responses were tested before and 30–40 min after superfusion of the cranial window with MK-801 (10 μM), recombinant tPA (rtPA (20 µg/ml; Genentech), the PAI-1 inhibitor PAI-039 (30 μM; Axon Medchem; Elokdah et al., 2004; Crandall et al., 2006; Hennan et al., 2008; Griemert et al., 2019), TTX (3 μM), or the cyclooxygenase-2 (COX-2) inhibitor NS-398 (100 μM) alone or in combination. The efficacy of the rescue of tPA activity in the neocortex was confirmed by using *in situ* zymography as shown previously (Park et al., 2008a). After testing CBF responses during Ringer's superfusion, the superfusion solution was changed to Ringer's solution (Iadecola, 1992, for composition) containing $A\beta_{1\text{-}40}$ (5 μM; rPeptide). This concentration of $A\beta_{1\text{-}40}$ was previously found to produce maximal cerebrovascular effects (Niwa et al., 2000a, 2001; Park et al., 2004). As in previous studies (Niwa et al., 2000a, 2001; Park et al., 2004), to minimize aggregation of the peptide during the experiment, $A\beta_{1\text{-}40}$ was freshly solubilized in dimethylsulfoxide (DMSO) and then diluted in Ringer's solution. The final DMSO concentration was $<0.5\%$ (Niwa et al., 2000a, 2001; Park et al., 2004). The CBF response to whisker stimulation, ACh, adenosine, NMDA, AMPA, TTX, tPA, or MK-801 alone or in combination was tested 30–40 min after $A\beta_{1\text{-}40}$ superfusion. This time interval was selected on the basis of previous studies in which the time course of the cerebrovascular effects of $A\beta_{1\text{-}40}$ was investigated (Park et al., 2004, 2005, 2017).

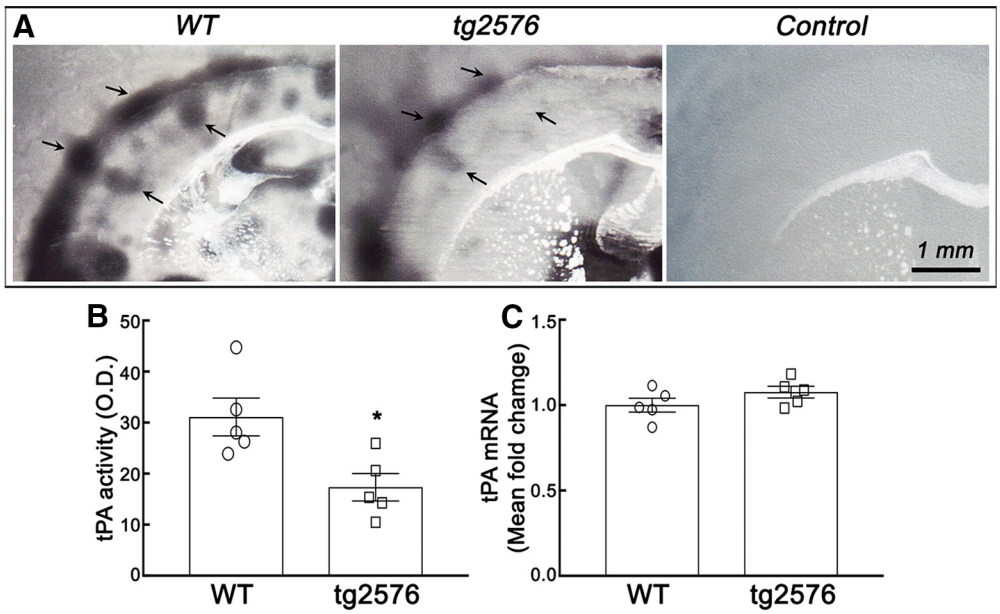

Figure 1. tPA activity is reduced in 3- to 4-month-old tg2576 mice. ***A***, Representative zymographic images show the dark lytic zones, indicated by dark arrows, of tPA activity from 3- to 4-month-old WT and tg2576 mice. Note no dark lytic zones in control image without plasminogen. ***B***, ***C***, Quantification of tPA activity (***B***) and tPA mRNA level (***C***) in WT and tg2576 mice. $N = 5$/group; $^*p = 0.0168$, unpaired two-tailed t test.

In situ *zymography*. *In situ* zymography was performed as described previously (Park et al., 2008a). Briefly, mice were deeply anesthetized and killed, and brains were removed and frozen at −80°C. In experiments with neocortical superfusion of tPA, the superfusion site was marked for later identification. Sections (20 μM) were cut through the superfusion site and mounted on microscope slides. A fresh casein gel was prepared with plasminogen (50 μg/ml) and overlaid on sections with a coverslip. Sections were allowed to develop at 37°C in a humidified chamber for 8 h. Zymographic lysis of casein produces a dark zone reflecting tPA activity. Images were digitized and quantified using ImageJ.

Real-time PCR for tPA. Total RNA was isolated from the forebrain tissue using TRIzol reagent (Thermo Fisher Scientific; Jackman et al., 2013). Quantitative determination of gene expression was performed on a Chromo 4 detector (Peltier thermal cycler, MJ Research) using a two-step cycling protocol. Primer sequences used for tPA (plat) were as follows: plat, forward, 5′-AATAAAACCGTCACGAACAACA-3′; and reverse, 5′-TTTATTGATCATGCACACCAGAG-3′. Two microliters of diluted cDNA (1:10) were amplified by Platinum SYBR green qPCR supermix UDG (Thermo Fisher Scientific). The reactions were incubated at 50°C for 2 min and then 95°C for 10 min. A PCR cycling protocol consisting of 15 s at 95°C and 1 min at 60°C for 45 cycles was required for quantification. Quantities of all targets in test samples were normalized to the mouse housekeeping hypoxanthine-guanine phosphoribosyltransferase (HPRT) gene (Jackman et al., 2013).

Quantification of PAI-1 activity by ELISA. To quantify PAI-1 activity in the brain, mice were anesthetized with 5% isoflurane and perfused with ice-cold PBS. Brains were removed and frozen with dry ice and saved in −80°C until assay. Then, PAI-1 activity was assessed in brain homogenates with a mouse PAI-1 activity ELISA kit (Molecular Innovations) according to the manufacturer instructions.

Electrocorticogram and field potentials. Mice were anesthetized as described above, and an electrocorticogram (ECG) was recorded by using bipolar recording electrodes positioned stereotaxically on the left somatosensory cortex (3 mm lateral and 1.5 mm caudal to bregma; depth of 0.6 mm; Park et al., 2008a, 2020). The ECG was recorded for five epochs each lasting 5 min and separated by a 20 min interval. The timing of the recordings relative to the administration of anesthesia was identical for all animals. Signals were amplified, digitized, and stored (PowerLab, AD Instruments). Spectral analysis of the EEG was performed by using a software module embedded in PowerLab. Field potentials were recorded by using an electrode placed in the somatosensory cortex contralateral to the activated whiskers. The somatosensory cortex was activated by electrical stimulation of the whisker pad (2 V; 0.5 Hz; pulse duration, 1 ms). Analyses were performed on the average of 10 stimulation trials.

Nitric oxide detection by DAF-FM in dissociated neocortical neurons. As detailed previously (Coleman et al., 2010; Wang et al., 2013), coronal cortical slices (thickness, 350 μm) were cut from the brains of 3- to 4-month-old WT and tg2576 mice and incubated with artificial CSF (aCSF; Coleman et al., 2010, for composition) containing Pronase 0.02% (w/v) and thermolysin 0.02% at 36°C (Sigma-Aldrich). Cortical neurons were mechanically dissociated for the assessment of NO production. Dissociated neurons were incubated with DAF-FM (5 μM) in oxygenated aCSF for 30 min, and then rinsed in control buffer (Coleman et al., 2010; Wang et al., 2013; Koizumi et al., 2018). The specificity of the NO detection by DAF-FM was verified by assessing the loss of NO signal after adding the non-selective NOS inhibitor N_ω-Nitro-L-arginine (100 μM) to the dishes (Coleman et al., 2010; Wang et al., 2013; Park et al., 2020). Time-resolved fluorescence (FITC filter) was measured at 30 s intervals with a Nikon diaphot 300 inverted microscope equipped with CCD digital camera (Princeton Instruments) connected to IPLab software (Scanalytics). In experiments with WT neurons, $A\beta_{1-40}$ (300 nM) was added for 30–40 min directly to the dish. In some experiments, neurons were pretreated with the tPA (20 μg/ml; Park et al., 2008a). DAF-FM fluorescence intensity is expressed as Ft/Fo, where Fo is the baseline fluorescence before application of NMDA (40 μM), and Ft is fluorescence in the same cell after the application of NMDA.

Chronic administration of PAI-039 into the cerebral ventricles. Osmotic minipumps (model 1004, Alzet) containing the PAI-1 inhibitor PAI-039 (Axon MedChem; Capone et al., 2011) or Ringer's solution served as a vehicle control and were implanted subcutaneously in 10- to 11-month-old tg2576 or WT littermates ($N = 11$/group) under isoflurane anesthesia. The osmotic minipump was connected to an intracerebroventricular catheter placed into the right ventricle at the following coordinates: anteroposterior, −0.22 mm; lateral, 0.8 mm; dorsal, 2 mm; Franklin and Paxinos, 1997). PAI-039 was delivered at a rate of 42 ng/kg/min (Elokdah et al., 2004; Crandall et al., 2006; Hennan et al., 2008; Griemert et al., 2019) for 4 weeks. PAI-039 was first dissolved in DMSO according to the manufacturer instruction and finally diluted in Ringer's solution (<0.5% of final DMSO). Three weeks after implanting the minipump, behavioral tests (Y-maze and novel object recognition test) were

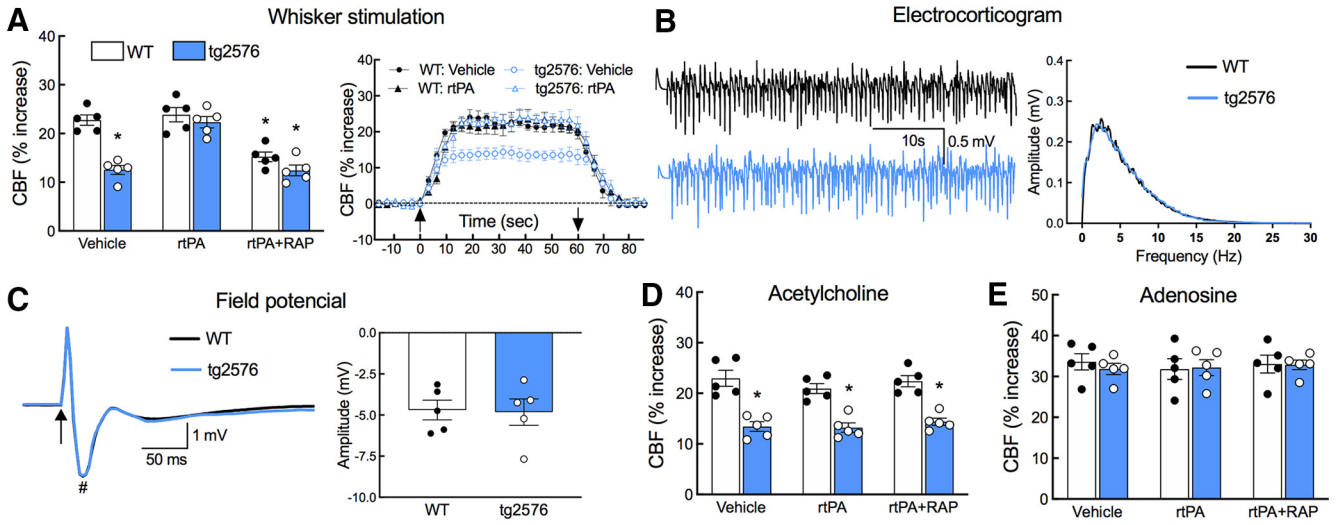

Figure 2. tPA deficiency is associated with selective attenuation in neurovascular coupling in 3- to 4-month-old tg2576 mice. ***A***, The increase in CBF induced by mechanical stimulation of facial whiskers is markedly attenuated in tg2576 mice compared with WT littermates. Neocortical superfusion with rtPA (20 μg/ml) completely rescues the CBF response, but it fails to do so in the presence of RAP (200 nM). Left, quantification graph; right, traces of CBF increase (percentage) induced by whisker stimulation. $*p \leq 0.0001$; two-way ANOVA with Tukey's test. ***B***, ***C***, Electrocorticogram (***B***) and evoked field potential (***C***) are comparable between WT and tg2576. #The amplitude of the negative deflection of the field potential is shown on the barograph on the right; $N = 5$/group. ***D***, ***E***, The increase in CBF induced by whisker barrel cortex superfusion of acetylcholine (***D***), but not by adenosine (***E***), is attenuated in tg2576 mice and is unaffected by rtPA or rtPA + RAP. $*p \leq 0.0015$ versus WT vehicle or rtPA; two-way ANOVA and Tukey's test. $N = 5$/group.

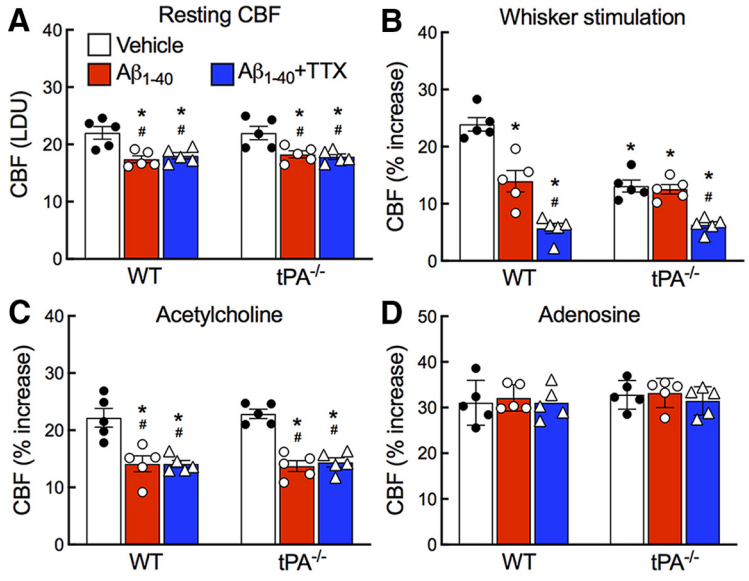

Figure 3. $A\beta_{1\text{-}40}$ does not attenuate functional hyperemia in $tPA^{-/-}$ mice. ***A–C***, In WT mice, neocortical superfusion with $A\beta_{1\text{-}40}$ (5 μM) attenuates resting CBF (***A***) and CBF increase produced by whisker stimulation (***B***) or neocortical application of acetylcholine (10 μM, ***C***). In $tPA^{-/-}$ mice, $A\beta_{1\text{-}40}$ fails to attenuate CBF increase produced by whisker stimulation (***B***), but it is still able to reduce resting CBF (***A***) or CBF increase to acetylcholine (***C***). ***A–D***, Coapplication with the Na^+ channel blocker TTX (3 μM) further reduces the CBF response to whisker stimulation in both $tPA^{-/-}$ and WT mice (***B***), but has no effect on resting CBF or CBF response to acetylcholine or adenosine (***A***, ***C***, ***D***). CBF response to adenosine is not affected by any treatment (***D***). LDU indicates laser-Doppler perfusion units; in ***A***, $*p \leq 0.0311$ versus WT vehicle, and $\#p \leq 0.0328$ versus $tPA^{-/-}$ vehicle; in ***B***, $*p < 0.0001$ versus WT vehicle and $\#p \leq 0.0084$ versus WT $A\beta_{1\text{-}40}$ or $tPA^{-/-}$ vehicle or $A\beta_{1\text{-}40}$; in ***C***, $*p \leq 0.0005$ versus WT vehicle and $\#p \leq 0.0002$ versus $tPA^{-/-}$ vehicle; two-way ANOVA and Tukey's test; $N = 5$/group.

performed. Some mice were prepared for *in situ* zymography as described above, and other mice were anesthetized and equipped for measurement of cerebrovascular reactivity by laser-Doppler flowmetry, as described above. At the end of CBF assessment, mice were killed, and the brains were removed. The left hemisphere was used for Aβ quantification by ELISA, and the right hemisphere was used for assessment of plaque burden and CAA.

Measurement of Aβ. Aβ was measured using an ELISA-based assay as described previously (Zhao et al., 2016). Briefly, the left hemispheres from the mice used for CBF studies were homogenated serially with RIPA and a 5.5 M guanidine buffer containing a cocktail of protease inhibitors (1:1000; Roche). Aβ measured after the RIPA extraction represented the soluble pool of Aβ, whereas Aβ measured after guanidine extraction represented the insoluble pool. The homogenates were diluted with a cold sample dilution buffer (1% bovine serum albumin in PBS and 0.05% Tween 20 [PBST]) before measurement of $A\beta_{1\text{–}40}$ or $A\beta_{1\text{–}42}$. Guanidine-solubilized samples were diluted with a cold sample dilution buffer to a final concentration of ≤0.5 M GuHCl. Samples were loaded onto plates coated with an antibody that specifically recognizes the C-terminal domain of $A\beta_{1\text{–}42}$ (21F12) or $A\beta_{1\text{–}40}$ (2G3) as the capture antibody, and biotinylated 3D6 was used for detection. The immunoreactivity signal after incubation with horseradish peroxidase-conjugated streptavidin (Research Diagnostics) was developed with a TMB substrate (Thermo Fisher Scientific) and read on a Synergy H1 Hybrid plate reader (BioTek). Levels of Aβ were calculated using a standard curve generated with recombinant human Aβ (American Peptide Company). Levels of Aβ in brain homogenates were determined in triplicate, normalized to protein content, and expressed as the amount of Aβ per milligram of protein. Concentrations in picomoles per milligram of brain tissue were calculated by comparing the sample absorbance with the absorbance of known concentrations of synthetic $A\beta_{1\text{–}40}$ and $A\beta_{1\text{-}42}$.

Quantification of amyloid plaque burden and cerebral amyloid angiopathy. Mice were deeply anesthetized and perfused transcardially with 4% PFA (Park et al., 2008b, 2013). Brain were sectioned (40 μm), and sections were processed with 0.05% (w/v) thioflavin-S in 50% (v/v)

ethanol for 10 min to quantify CAA and amyloid burden. Confocal images were obtained with an FITC filter for thioflavin-S. Images of thioflavin-S staining were acquired with a confocal microscope (Leica SP8) and quantified by ImageJ, and CAA and Aβ plaque burden were expressed by thioflavin-S-positive neocortical vessels (Thio-S$^+$ CAA; as a percentage) or Aβ load (Thio-S$^+$ plaques area; as a percentage), respectively (Park et al., 2008b, 2013).

Cognitive testing. Cognitive testing was performed by the Y-maze and novel object recognition test. These tests were used because of the following: (1) they are sensitive to the cognitive deficits in tg2576 mice (Park et al., 2008b, 2013; Faraco et al., 2018; Koizumi et al., 2018); (2) they rely on the spontaneous behavior of mice; and (3) they do not require aversive environments, such as for training or starvation of the mice (Dellu et al., 2000; Wenk, 2004; Vorhees and Williams, 2014).

Y-maze spontaneous alternation behavior. Mice were placed into one of the arms of the maze (start arm) and were allowed to explore only two of the three arms for 5 min (training trial). The closed arm was opened in the test trial, serving as the novel arm. After a 30 min interval between trials, the mice were returned to the same start arm and were allowed to explore all three arms for 5 min (test trial). Sessions were video recorded and analyzed using AnyMaze (San Diego Instruments) in a double-blinded fashion. Spontaneous alternation was evaluated by scoring the order of entries into each arm during the 5 min of the test trial. Spontaneous arm alternation (percentage) was defined as follows: number of arm alternations/(total number of arm visits-2) × 100.

Novel object recognition. The test was performed in 2 consecutive days. On day 1, mice were placed in the center of an empty open box and allowed to explore for 5 min. The box was cleaned with 70% ethanol between trials. On day 2, the mice were placed back into an open box with two identical objects in the center and allowed to explore for 5 min. Thirty minutes later, mice were exposed again to a familiar and a novel object, and allowed to explore for 5 min. The exploring activity (facing, touching, or sniffing the object) was monitored and analyzed using AnyMaze in a double-blinded manner, and the percentage of the time spent exploring the novel versus familiar objects was calculated.

Data analysis. Statistical analysis was performed using GraphPad Prism (GraphPad Software). Immunofluorescent staining analyses were conducted in a blinded fashion. Samples and animals were randomized by a random number generator (www.random.org). The number of mice required for assessing the statistical significance of prespecified effects was estimated by power analysis based on preliminary results and previous experience with the models used in the laboratory. Normality was tested using D'Agostino–Pearson normality test (GraphPad Prism) before running appropriate statistical tests. Two-group comparisons were analyzed by the two-tailed *t* test, and multiple comparisons were evaluated by one-way or two-way ANOVA with Tukey's test, as required, after testing for equality

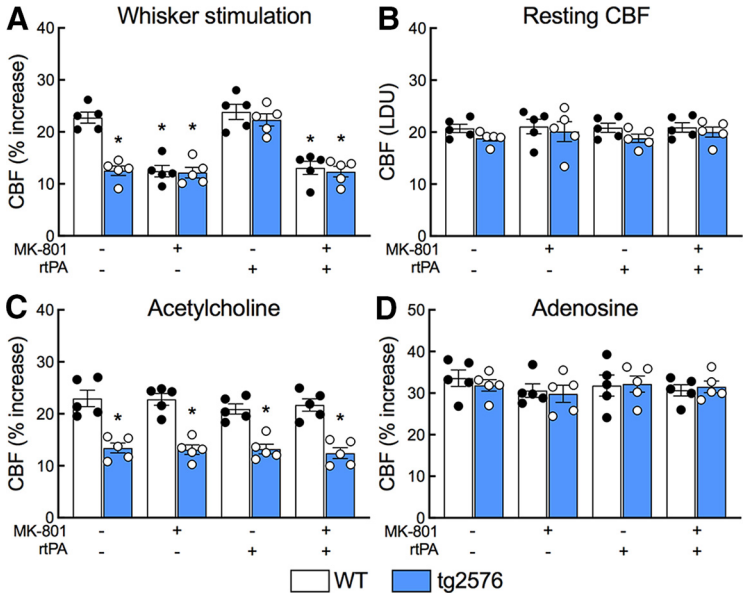

Figure 4. tPA deficiency is associated with Aβ-induced reduction in the NMDA receptor-dependent component of functional hyperemia in 3- to 4-month-old tg2576 mice. ***A***, Neocortical superfusion with the NMDAR antagonist MK-801 (10 μM) attenuates the CBF increase evoked by whisker stimulation in WT mice and not in tg2576 mice. In addition, rtPA fails to rescue the neurovascular dysfunction in the presence of MK-801. ***B–D***, Treatment with MK-801 and/or rtPA does not affect resting CBF (***B***) or the CBF response to superfusion of acetylcholine (***C***) or adenosine (***D***). LDU indicates laser-Doppler perfusion units; in ***A***, *$p < 0.0001$ versus WT no treatment, WT rtPA, or tg2576 rtPA; in ***C***, *$p \leq 0.0001$ versus WT; two-way ANOVA and Tukey's test; $N = 5$/group.

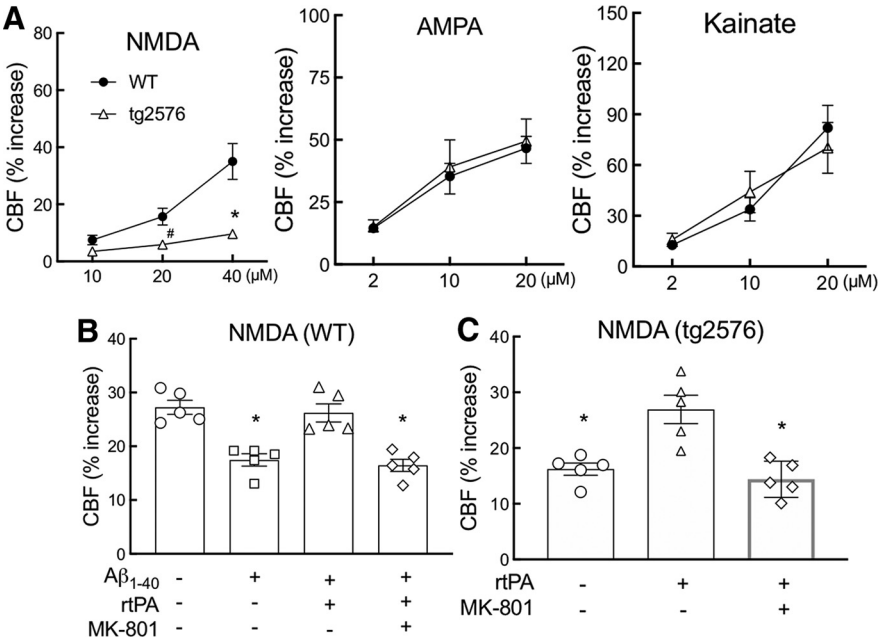

Figure 5. tPA rescues the attenuation of the hyperemic response induced by NMDA in Aβ. ***A***, The increase in CBF produced by neocortical application of NMDA, but not AMPA or kainate, is attenuated in 3- to 4-month-old tg2576 mice, compared with age-matched WT mice. #$p = 0.0164$ or *$p < 0.0038$ versus the same does of WT; two-way ANOVA with Tukey's test; $N = 5$/group. ***B***, Neocortical application of A$\beta_{1\text{-}40}$ (5 μM) attenuates the CBF increase induced by NMDA in WT mice. Pretreatment with rtPA (20 μg/ml) reverses the effect of A$\beta_{1\text{-}40}$ on the NMDA-induced CBF increase, but it fails to do so in the presence of MK-801 (10 μM). *$p \leq 0.0014$ versus no treatment or A$\beta_{1\text{-}40}$ + rtPA; one-way ANOVA with Tukey's test (***B***). ***C***, rtPA rescues the CBF response to NMDA in tg2576 mice, an effect abolished by pretreatment with MK-801. *$p \leq 0.0033$ versus rtPA; one-way ANOVA with Tukey's test. $N = 5$/group.

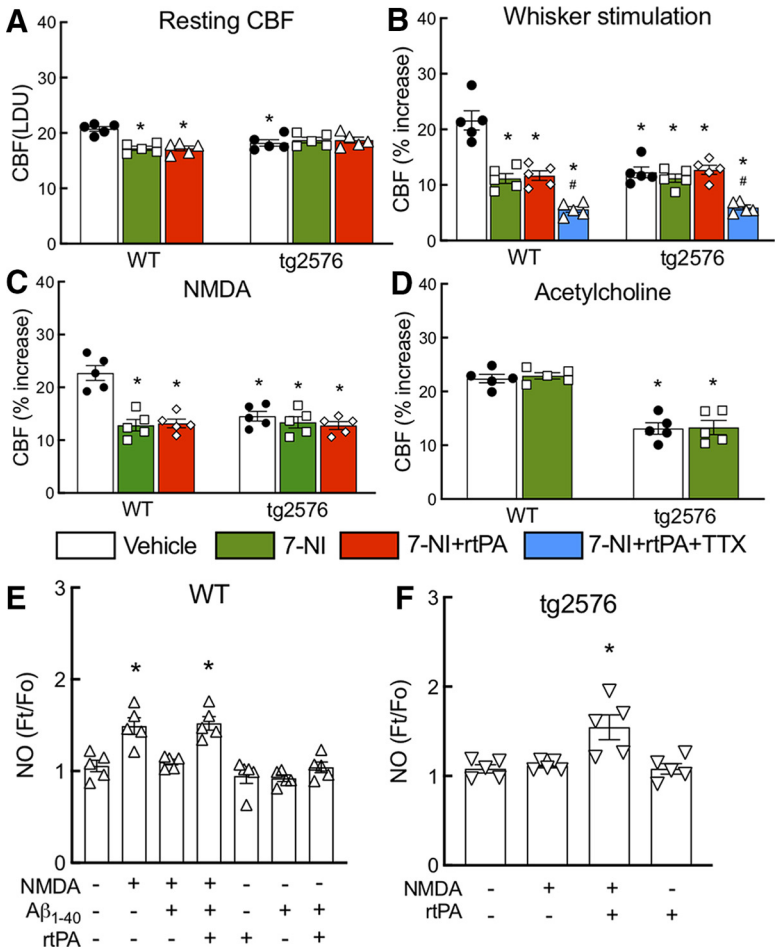

Figure 6. tPA deficiency is responsible for the attenuation in the NOS-dependent component of functional hyperemia and for the attenuation in NMDA-dependent NO production induced by exogenous Aβ and in tg2576 mice. ***A–D***, Administration of the nNOS inhibitor 7-NI (50 mg/kg, i.p.) attenuates resting CBF (*$p \leq 0.0127$ vs WT vehicle; ***A***) and the increase in CBF produced by whisker stimulation (*$p \leq 0.0001$ vs WT vehicle; ***B***) or by neocortical application of NMDA (40 μM; *$p < 0.0001$ vs WT vehicle; ***C***) in WT mice, but not in tg2576 mice. 7-NI has no effect on the CBF increase induced by acetylcholine (10 μM) both in WT and tg2576 mice (*$p < 0.0001$ vs WT; ***D***). The Na^+ channel blocker TTX (3 μM) further reduces CBF responses to whisker stimulation in both WT and tg2576 mice (#$p \leq 0.0101$ vs 7-NI- or 7-NI + rtPA-treated WT or tg2576 mice; ***B***). ***E***, ***F***, NMDA (40 μM) increases NO production in cortical neurons dissociated from 3- to 4-month-old WT mice (***E***), but not in neurons from tg2576 mice (***F***). NMDA-induced NO production in WT neuron is attenuated by pretreatment of A$\beta_{1\text{-}40}$ (300 nM; ***E***). rtPA (20 μg/ml) treatment rescues the attenuation of NO production induced by A$\beta_{1\text{-}40}$ in WT neurons (***E***) and in tg2576 mice (***F***). LDU indicates laser-Doppler perfusion units; in ***A–D***, two-way ANOVA and Tukey's test; ***E***, ***F***, *$p \leq 0.0076$, one-way ANOVA and Tukey's test. $N = 5$/group.

of variance. Differences were considered statistically significant for probability values <0.05. Data are expressed as the mean ± SEM.

Results

tPA deficiency underlies the attenuation of functional hyperemia induced by Aβ

To assess whether tPA plays a role in the neurovascular dysfunction of Aβ, we first assessed tPA enzymatic activity using *in situ* zymography. We found that tPA activity is significantly reduced in 3- to 4-month-old tg2576 mice compared with WT littermates, whereas tPA mRNA levels were not reduced (Fig. 1*A–C*). Next, we examined neurovascular coupling in the somatosensory cortex of 3- to 4-month-old tg2576 mice. At this age, tg2576 mice exhibit increased levels of brain Aβ, but do not have plaques or CAA (Park et al., 2011, 2014, 2017). We found that the increase in CBF induced by mechanical stimulation of facial whiskers is markedly attenuated in tg2576 mice compared with WT littermates (Fig. 2*A*). Such attenuation was not because of suppression of the neural activity driving the hemodynamic response since the frequency distribution of the electrocorticogram and the amplitude of the somatosensory cortex field potentials evoked by stimulation of the whisker pad were similar in tg2576 and WT mice (Fig. 2*B*,*C*).

To determine whether the attenuation in neurovascular coupling observed in tg2576 mice was related to a deficiency in tPA, we investigated whether exogenous tPA could improve the response. Neocortical superfusion with rtPA (20 μg/ml), a dose previously shown to restore cortical tPA activity and neurovascular coupling in $tPA^{-/-}$ mice (Park et al., 2008a), re-established in full the CBF increase produced by whisker stimulation in tg2576 mice without affecting the response in WT mice (Fig. 2*A*). The effect was prevented by pretreatment with RAP, an inhibitor of the LRP1 (Fig. 2*A*), which has been implicated in the signaling between extracellular tPA and NMDAR (Herz, 2001; Samson and Medcalf, 2006). Notably, tPA did not rescue the CBF increase induced by topical application of the endothelium-dependent vasodilator acetylcholine (Fig. 2*D*). CBF responses to the smooth muscle relaxant adenosine were not altered in tg2576 mice and were not affected by rtPA, providing evidence for the stability of the preparation (Fig. 2*E*). These data, collectively, indicate that the deficit of tPA in tg2576 mice contributes to the attenuation of the increases in CBF evoked by neural activity, but not by the endothelium.

Aβ does not attenuate functional hyperemia in $tPA^{-/-}$ mice

Mice lacking tPA have reduced functional hyperemia, but a normal CBF response to acetylcholine (Park et al., 2008a; Iadecola, 2017; Anfray et al., 2020). We reasoned that if the suppression of neurovascular coupling by Aβ is because of a deficiency in tPA, then in tPA-null mice Aβ should not attenuate further the CBF response to whisker stimulation but should still reduce the response to acetylcholine. Consistent with this prediction, superfusion of somatosensory cortex with A$\beta_{1\text{-}40}$ (5 μM) failed to attenuate the CBF increase produced by whisker stimulation in $tPA^{-/-}$ mice, but was still able to reduce resting CBF and the CBF response to acetylcholine (Fig. 3*A–C*). To exclude the possibility that the failure of A$\beta_{1\text{-}40}$ to reduce neurovascular coupling further in $tPA^{-/-}$ mice was a consequence of the response being already maximally attenuated, we tested the effect of neocortical superfusion with TTX, a sodium channel inhibitor that suppresses neurovascular coupling by blocking synaptic transmission (Yang et al., 1999; Park et al., 2005). As shown in Figure 3*A–C*, treatment with TTX after A$\beta_{1\text{-}40}$ attenuated the CBF

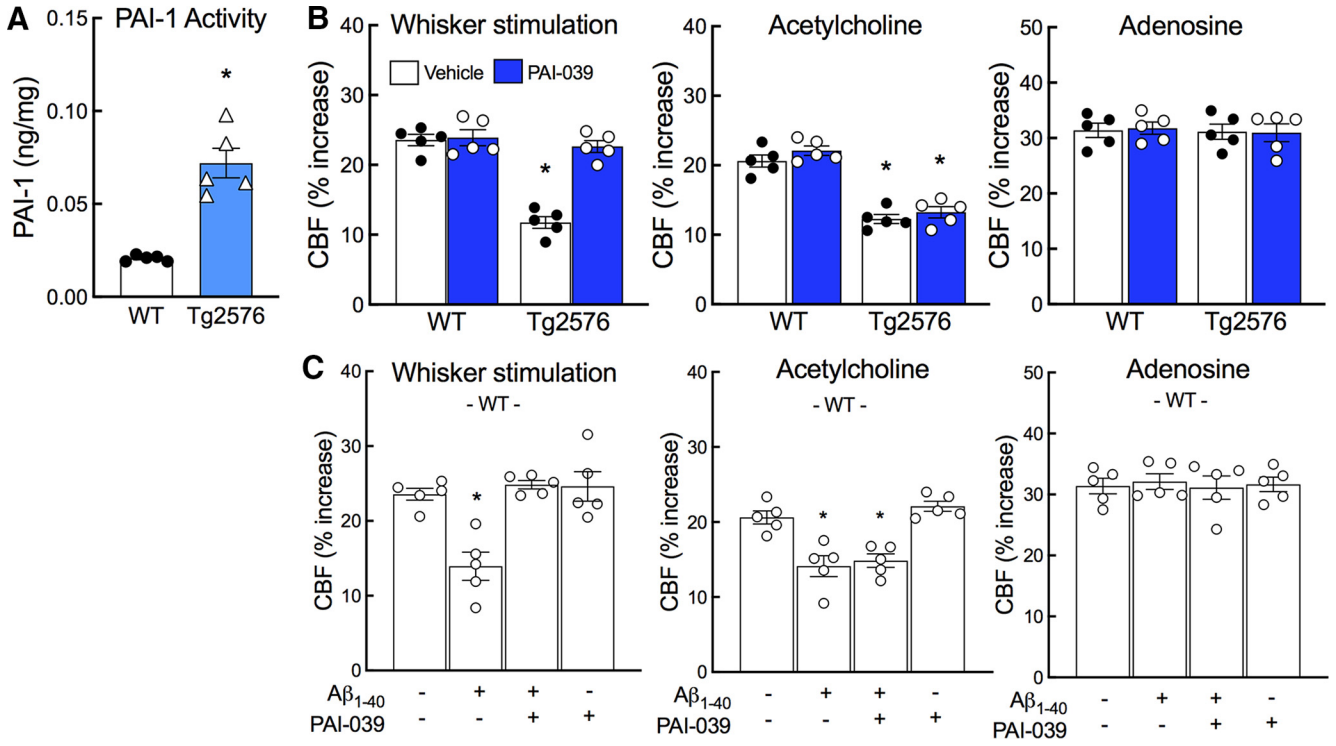

Figure 7. The PAI-1 inhibitor PAI-039 prevents Aβ-induced neurovascular coupling dysfunction. ***A***, PAI-1 activity is increased in 3- to 4-month-old tg2576 mice, compared with age-matched WT controls. *$p = 0.0002$; unpaired two-tailed *t* test. ***B***, ***C***, Topical neocortical application of the PAI-1 inhibitor PAI-039 (30 μM) rescues the attenuation in CBF increase produced by whisker stimulation in tg2576 mice (***B***) or induced by A$\beta_{1\text{-}40}$ in WT mice (***C***). In contrast, PAI-039 has no effect on CBF response to acetylcholine or adenosine both in tg2576 and WT mice (***B***, ***C***). In ***B*** and ***C***, *$p \leq 0.0042$, two-way ANOVA and Tukey's test. $N = 5$/group.

response to whisker stimulation further without reducing the response to acetylcholine both in tPA$^{-/-}$ and WT mice. These findings indicate that A$\beta_{1\text{-}40}$ is unable to attenuate neurovascular coupling in the absence of tPA but is still able to suppress endothelium-dependent responses.

tPA deficiency contributes to the suppression of the NMDAR-dependent component of the CBF response caused by Aβ

Activation of NMDAR is responsible for ~50% of the flow increase induced by whisker stimulation in the somatosensory cortex (Iadecola, 2017). Because tPA is required for the full expression of the NMDAR-dependent component of the CBF increase (Park et al., 2008a), it is conceivable that in tg2576 mice tPA deficiency specifically suppresses the fraction of the response mediated by NMDAR. In this case, NMDAR inhibition should not attenuate further neurovascular coupling in tg2576 mice, and tPA should not reverse the attenuation if NMDARs are inhibited. Accordingly, we found that the NMDAR antagonist MK-801 reduces the CBF response produced by whisker stimulation in WT mice, but not in tg2576 mice (Fig. 4*A*), without affecting resting CBF and other cerebrovascular responses (Fig. 4*B–D*). In addition, MK-801 prevented tPA from reestablishing neurovascular coupling in tg2576 mice (Fig. 4*A*).

To more directly examine the role of tPA deficiency on the suppression of NMDAR-dependent hyperemia in tg2576 mice, we examined the neurovascular effects of the application of NMDA to the somatosensory cortex. The CBF increase induced by NMDA (10–40 μM), but not AMPA or kainate (2–20 μM), was profoundly reduced in tg2576 mice compared with WT littermates (Fig. 5*A*). Furthermore, rtPA was able to re-establish the CBF response both in tg2576 and in WT mice with neocortical superfusion of A$\beta_{1\text{-}40}$, an effect prevented by MK-801 (Fig. 5*B*,*C*). These findings indicate that Aβ suppresses the NMDAR-dependent component of functional hyperemia because of a deficit in tPA.

tPA deficiency contributes to the suppression of NMDAR-dependent NO production induced by Aβ

Next, we sought to investigate the pathways by which tPA deficiency lead to the attenuation of NMDAR-dependent CBF response induced by Aβ. Because tPA promotes the CBF response initiated by NMDAR by enabling NO production from the neuronal isoform of NO synthase (nNOS; Park et al., 2008a; Iadecola, 2017), we reasoned that NOS inhibition would prevent tPA from rescuing neurovascular coupling. In WT mice, as anticipated, the nNOS inhibitor 7-nitroindazole (7-NI; 50 mg/kg, i.p.) attenuated resting CBF and the CBF increases evoked by whisker stimulation or neocortical application of NMDA, but not acetylcholine, a response mediated by the endothelial isoform of NOS (Fig. 6*A–D*). In contrast, in tg2576 mice 7-NI did not reduce resting CBF and the CBF responses to whisker stimulation or topical NMDA (Fig. 6*A–C*). Furthermore, rtPA failed to rescue neurovascular coupling after nNOS inhibition (Fig. 6*B*, *C*), whereas TTX further decreased the response to whisker stimulation (Fig. 6*B*), confirming that it was not maximally attenuated.

To investigate whether Aβ suppresses NMDAR-dependent NO production through tPA deficiency, we assessed NO production in dissociated neocortical neurons using DAF-FM as an indicator (Coleman et al., 2010; Wang et al., 2013). We found that NMDA (40 μM) was able to increase NO in WT neurons, but not in WT neurons pretreated with A$\beta_{1\text{-}40}$ (300 nM) or in neurons from tg2576 mice (Fig. 6*E*,*F*). rtPA was able to completely re-establish NMDA-induced NO production both in WT neurons exposed

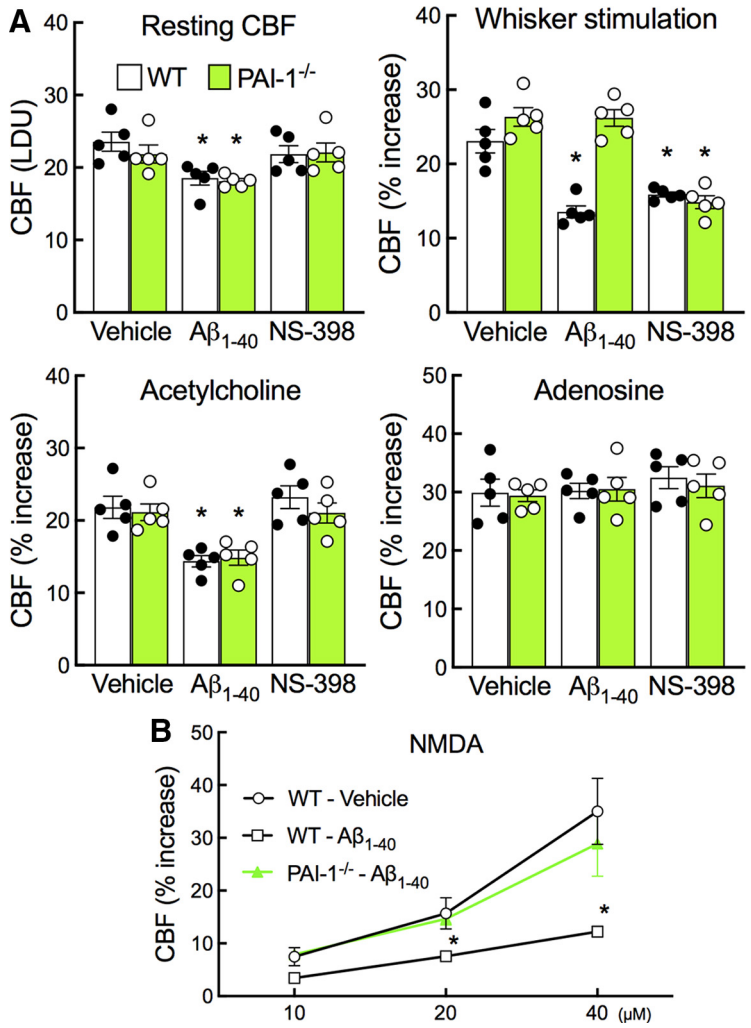

Figure 8. $A\beta_{1\text{-}40}$ does not suppress functional hyperemia in PAI-$1^{-/-}$ mice, but reduces the endothelium-dependent response to acetylcholine. ***A***, $A\beta_{1\text{-}40}$ (5 μM) does not attenuate functional hyperemia in PAI-$1^{-/-}$ mice. However, the response to topical application of acetylcholine is attenuated by $A\beta_{1\text{-}40}$. The COX-2 inhibitor NS-398 (100 μM) is able to attenuate the CBF increase induced by whisker stimulation both in PAI-$1^{-/-}$ and WT mice but has no effect on other CBF responses. CBF responses to adenosine are unaffected. *$p \leq 0.0391$, two-way ANOVA and Tukey's test. ***B***, $A\beta_{1\text{-}40}$ attenuates CBF increase induced by topical application of NMDA in WT, but not in PAI-$1^{-/-}$ mice, compared with vehicle-treated WT. LDU indicates laser-Doppler perfusion units; *$p \leq 0.0197$ versus WT-vehicle or PAI-$1^{-/-}$-$A\beta_{1\text{-}40}$ at the same dose; two-way ANOVA and Tukey's test. Data are presented as the mean ± SEM. $N = 5$/group.

to $A\beta_{1\text{-}40}$ and in tg2576 neurons (Fig. 6*E*,*F*). These findings, collectively, suggest that $A\beta$ suppressed the NMDAR-dependent component of function hyperemia by suppressing nNOS-dependent NO production and that tPA deficiency is involved in this effect.

PAI-1 inhibition ameliorates the neurovascular coupling dysfunction induced by Aβ

Since the endogenous tPA inhibitor PAI-1 is upregulated in AD and in APP-overexpressing mice (Melchor et al., 2003; Cacquevel et al., 2007; Jacobsen et al., 2008; Hanzel et al., 2014; Oh et al., 2014), we sought to determine whether inhibiting PAI-1 can reverse the neurovascular dysfunction induced by $A\beta$. In agreement with previous studies (Melchor et al., 2003; Jacobsen et al., 2008), PAI-1 activity was elevated in tg2576 mice compared with age-matched WT mice (Fig. 7*A*), a finding consistent with the observed tPA deficiency (Fig. 1). Neocortical superfusion of the PAI-1 inhibitor PAI-039 (30 μM) did not affect CBF responses in WT mice, but completely rescued the attenuation in functional hyperemia either in tg2576 mice or in WT mice treated with $A\beta_{1\text{-}40}$ superfusion (Fig. 7*B*,*C*). PAI-039 did not affect CBF responses to acetylcholine or adenosine both in WT and tg2576 mice (Fig. 7*B*,*C*).

To provide nonpharmacological evidence that PAI-1 is involved in the neurovascular dysfunction induced by $A\beta$, we studied the vascular effect of $A\beta_{1\text{-}40}$ in PAI-1-deficient mice. CBF responses to whisker stimulation or to neocortical application of acetylcholine or adenosine were comparable between PAI-$1^{-/-}$ and WT mice (Fig. 8*A*). In PAI-$1^{-/-}$ mice, $A\beta_{1\text{-}40}$ attenuated resting CBF and the CBF response to acetylcholine but did not suppress the increase in CBF evoked by whisker stimulation (Fig. 8*A*) or by neocortical superfusion of NMDA (Fig. 8*B*). In contrast, the inhibition of COX-2, an enzyme involved in neurovascular coupling independently of NO (Niwa et al., 2000b), attenuated the CBF response to whisker stimulation in both WT and PAI-$1^{-/-}$ mice (Fig. 8*A*), confirming the specific role of PAI-1 in the neurovascular dysfunction resulting from tPA deficiency.

Sustained restoration of tPA activity by PAI-1 inhibition ameliorates neurovascular and cognitive dysfunction in aged tg2576 mice

To examine the contribution of tPA deficiency to amyloid pathology and cognitive deficits, we investigated tg2576 mice at an age (11–12 months) when there is amyloid deposition in brain and blood vessels (Park et al., 2008b). To this end, PAI-039 was administered intracerebroventricularly for 4 weeks in aged tg2576 mice at a concentration (42 ng/kg/min) previously shown to suppress PAI-1 activity *in vivo* (Elokdah et al., 2004; Crandall et al., 2006). PAI-039 increased tPA activity in tg2576 mice to levels comparable to WT controls (Fig. 9*A*, but see Fig. 1). Then, we determined whether rescuing tPA activity by PAI-1 inhibition also improves neurovascular dysfunction in aged tg2576 mice. In vehicle-treated tg2576 mice, CBF responses to whisker stimulation, already attenuated at 3–4 months of age, became worse at 11–12 months of age (Fig. 9*B*). Treatment with PAI-039 markedly improved the response in aged tg2576 mice (Fig. 9*B*), congruent with the rescue of tPA activity (Fig. 9*A*).

Next, we investigated whether PAI-1 inhibition reduces brain $A\beta$ accumulation and ameliorates the cognitive dysfunction in aged tg2576 mice. PAI-039 treatment reduced the levels of $A\beta_{1\text{-}40}$, not $A\beta_{1\text{-}42}$, in the cortex and hippocampus of 11- to 12-month-old tg2576 mice (Fig. 9*D*,*E*). Consistent with the predominant accumulation of $A\beta_{1\text{-}40}$ around blood vessels (CAA) and $A\beta_{1\text{-}42}$ in amyloid plaques (Greenberg et al., 2020), PAI-039 treatment reduced CAA, but not amyloid plaques (Fig. 9*F*). We then examined whether the improvement in neurovascular

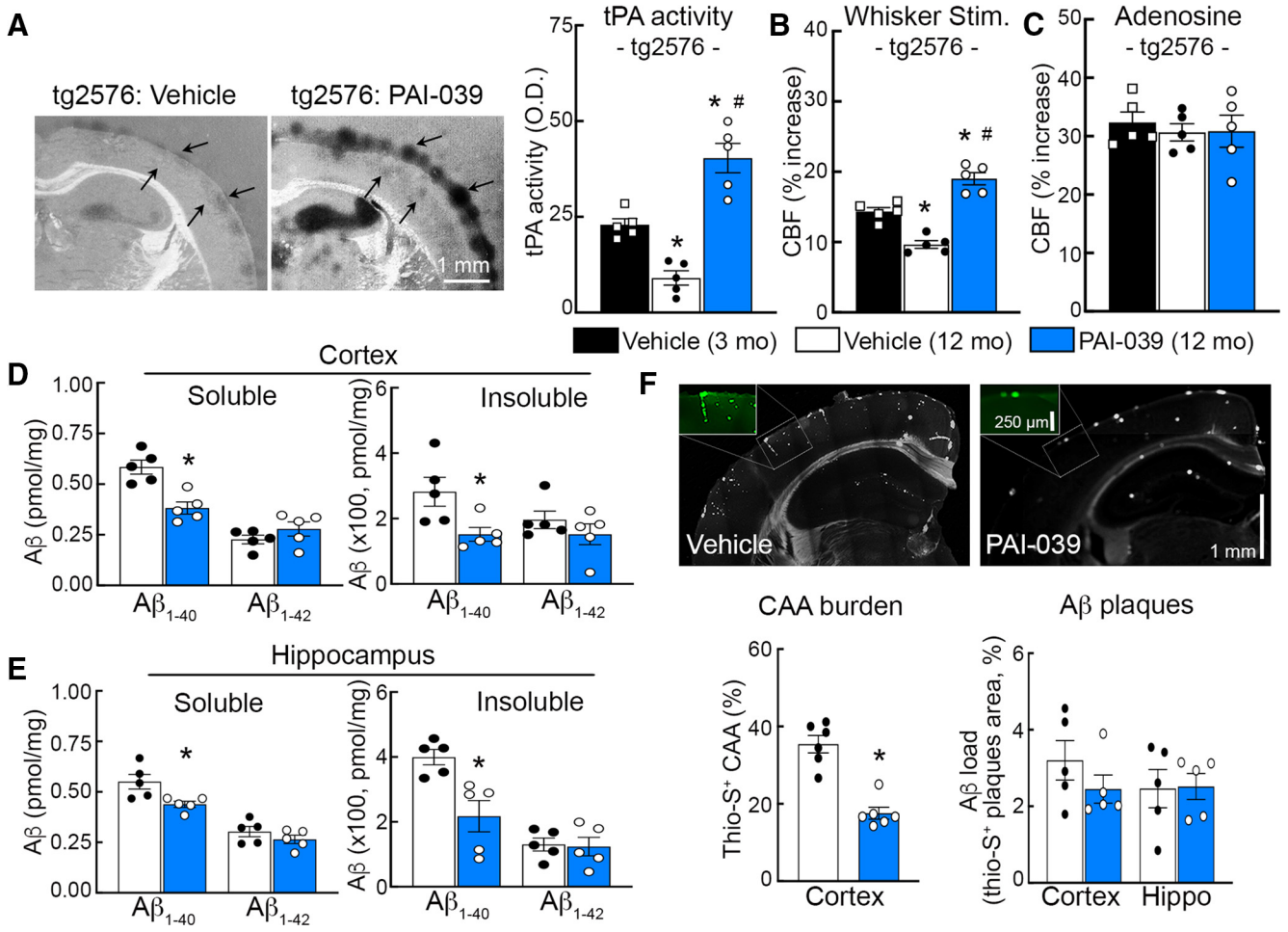

Figure 9. PAI-1 inhibition reverses neurovascular dysfunction, reduces A$\beta_{1\text{-}40}$ level, and attenuates CAA, but not Aβ plaques, in 11- to 12-month-old tg2576 mice. ***A***, Intracerebroventricular administration of the PAI-1 inhibitor PAI-039 for 4 weeks rescues tPA activity, assessed by *in situ* zymography, in 11- to 12-month-old tg2576 mice. *$p \leq 0.0105$ versus vehicle (3 months); #$p = 0.0001$ versus vehicle (12 months); one-way ANOVA and Tukey's test. ***B***, It also improves the CBF response to whisker stimulation (Stim.). *$p \leq 0.0011$ versus vehicle (3 months); #$p < 0.0001$ versus vehicle (12 months); one-way ANOVA and Tukey's test. ***C***, The CBF response to adenosine is not affected. ***D***, ***E***, In addition, it attenuates levels of soluble and insoluble A$\beta_{1\text{-}40}$, but not A$\beta_{1\text{-}42}$, in cortex (***D***) and hippocampus (***E***). ***F***, The burden of CAA is reduced in the cortex, but amyloid plaques are not reduced. In ***D–F***, *$p \leq 0.0292$, one-way ANOVA and Tukey's test. $N = 5$/group.

function and reduced CAA caused by PAI-1 inhibition is associated with improved cognitive function in aged tg2576 mice. We first used a two-trial working memory task in a Y-maze (Park et al., 2008b; Spellman et al., 2015). In vehicle-treated tg2576 mice, the percentage of arm alternation was significantly attenuated, compared with vehicle-treated WT littermates (Fig. 10*A*). PAI-039 did not affect arm alternation behavior in WT mice, but it markedly improved task performance in tg2576 mice (Fig. 10*A*). To provide further evidence that reduced tPA plays a role in the cognitive deficits, we used the novel object recognition task (Leger et al., 2013; Koizumi et al., 2018). In vehicle-treated tg2576 mice, the preference for novel objects was markedly reduced compared with age-matched WT mice, but it was preserved in PAI-039-treated tg2576 mice (Fig. 10*B*). The locomotor activity was elevated in tg2576 mice, but it was not affected by PAI-039 (Fig. 10*C*,*D*). Therefore, restoring tPA activity by PAI-1 inhibition prevents the neurovascular dysfunction, reduces CAA, and improves the cognitive deficit in aged tg2576 mice.

Discussion

We have demonstrated that the reduction in tPA activity leads to suppression of the component of functional hyperemia mediated by NO released during NMDAR activation. The deficiency in tPA is because of increased PAI-1 enzymatic activity, and suppressing PAI-1 prevents the Aβ-induced attenuation of neurovascular coupling, but not the endothelial dysfunction. Prolonged inhibition of PAI-1 in aged tg2576 mice restores tPA activity, normalizes neurovascular coupling, and ameliorates cognitive dysfunction, effects associated with reduced CAA but not amyloid plaques (Fig. 11). These observations implicate tPA deficiency in the neurovascular and cognitive dysfunction induced by Aβ, and in the mechanisms of CAA as well.

Aβ impairs endothelium-dependent relaxation (Thomas et al., 1996), reduces resting CBF (Niwa et al., 2002a), dampens neurovascular coupling (Niwa et al., 2000c; Tong et al., 2012; Nortley et al., 2019), and alters the ability of cerebral blood vessels to regulate CBF independently of arterial pressure (cerebrovascular autoregulation; Niwa et al., 2002b). As in mouse models, cerebrovascular alterations have also been described in presymptomatic individuals at genetic risk for AD, as well as in people with sporadic AD early in the disease (Iadecola, 2013; Iturria-Medina et al., 2016; Chandler et al., 2019). The cerebrovascular effects of Aβ have been linked to reactive oxygen species (ROS) generated by perivascular macrophages, innate immune cells associated with cerebral blood vessels, in response

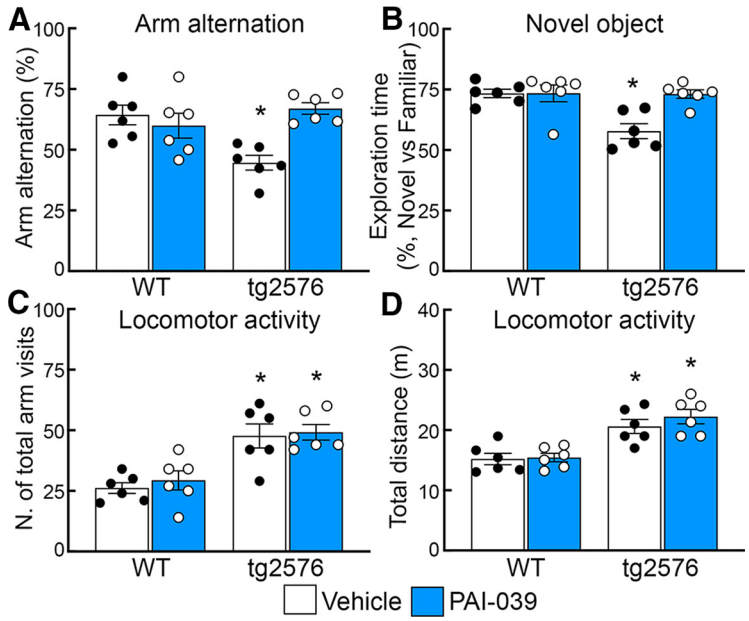

Figure 10. PAI-1 inhibition improves cognitive deficits in aged tg2576 mice. ***A–D***, In 11- to 12-month-old tg2576 mice, intracerebroventricular administration of the PAI-1 inhibitor PAI-039 improves cognitive deficits assessed by arm alternation in Y-maze (***A***; $*p \leq 0.0452$) or novel object recognition test (***B***; $*p \leq 0.0027$) without affecting locomotor activity in both tests (***C***, number of total arm visits in Y-maze; ***D***, total distance in novel object recognition test). In ***C*** and ***D***, $*p \leq 0.0112$ versus WT. Two-way ANOVA and Tukey's test. $N = 6$/group.

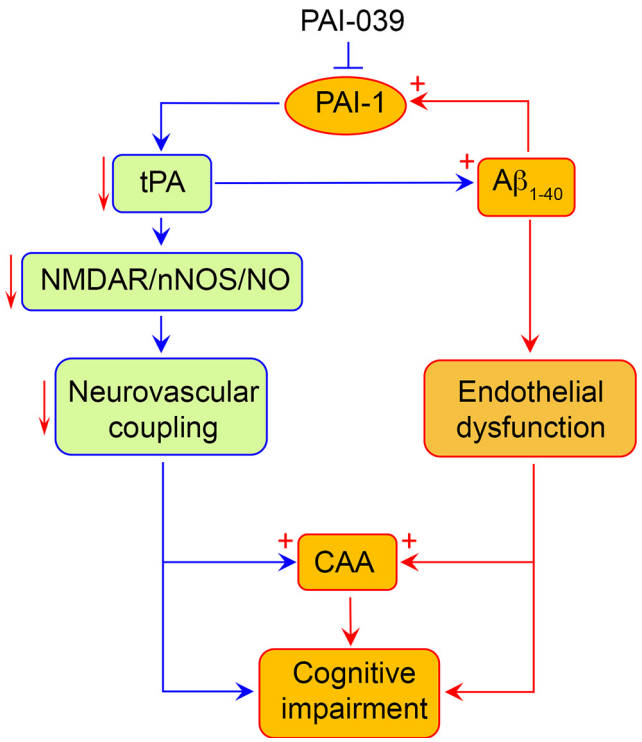

Figure 11. Putative mechanisms by which the tPA deficit caused by Aβ alters neurovascular coupling and cognition. Aβ increases PAI-1 activity, possibly through ROS. The resulting deficit in tPA reduces NMDA-dependent NO production during neural activity, disrupts neurovascular coupling (Fig. 1), and may promote Aβ accumulation (Fig. 9). Aβ also induces endothelial dysfunction through mechanisms independent of tPA. Neurovascular uncoupling and endothelial dysfunction could promote CAA by reducing Aβ vascular clearance. The combined effect of cerebrovascular dysfunction and CAA may lead to cognitive impairment. Inhibiting PAI-1 activity with PAI-039 improves deficits in neurovascular coupling, CAA, and cognition in tg2576 mice.

to activation of the scavenger receptor CD36 (Faraco et al., 2017; Park et al., 2017). In particular, the endothelial dysfunction is mediated by peroxynitrite formed by the reaction of superoxide with NO, leading to poly-ADP-ribose polymerase activation, generation of ADP-ribose, opening of the TRPM2 channel by ADP-ribose, and Ca^{2+} overload in endothelial cells (Park et al., 2014). However, the mechanisms of neurovascular uncoupling have remained unclear (Cortes-Canteli and Iadecola, 2020). Here we found that the deficit in tPA activity is responsible specifically for the suppression of neurovascular coupling induced by Aβ. First, exogenous tPA can normalize functional hyperemia, but not the endothelial dysfunction, in tg2576 mice or in WT mice with neocortical application of Aβ. Second, Aβ does not impair functional hyperemia in tPA-null mice, but it induces endothelial dysfunction, pointing to tPA being involved only in neurovascular uncoupling. Third, since the deficit in tPA results from increased PAI-1 activity, PAI-1 inhibition rescues the neurovascular dysfunction in tg2576 mice and in WT mice treated with Aβ, whereas Aβ does not alter functional hyperemia in PAI-1-null mice. PAI-1 genetic deletion or inhibition does not prevent Aβ from causing endothelial dysfunction. These observations link Aβ-induced neurovascular uncoupling specifically to the PAI-1–tPA pathway and reveal for the first time a mechanistic diversity in the impact of Aβ on the factors regulating the cerebral microcirculation.

Functional hyperemia is mediated by a wide variety of vasoactive agents targeting different segments of the cerebrovascular tree (Iadecola, 2017). Of these, NO derived from NMDAR activity mediates a significant fraction of the response, and tPA is required for the full expression of this component by enabling NO production during NMDAR activation (Park et al., 2008a; Anfray et al., 2020). Here, we found that the deficit in tPA attenuates functional hyperemia by suppressing the NMDAR-NO-mediated component of the response. Thus, the reduction in tPA caused by Aβ dampens NMDAR-induced NO production by nNOS, attenuating the rise in CBF evoked by neural activity.

How does tPA modulate NMDAR signaling? Some studies have indicated that tPA modulates Ca^{2+} influx through NMDAR by cleaving the extracellular domain of the GluN1 subunit (Nicole et al., 2001). Other studies have suggested that tPA does not act on NMDAR directly. Rather, tPA may signal through LRP1 (Martin et al., 2008; Samson et al., 2008; Mantuano et al., 2013), which, like nNOS, is bridged to the NMDA receptor complex through the adaptor protein PSD-95 (Gotthardt et al., 2000; May et al., 2004; Nakajima et al., 2013). The association of LRP1 with the NMDAR–PSD–nNOS complex is consistent with findings that tPA promotes the association between the NMDA receptor subunit GluR2B and PSD-95 (Norris and Strickland, 2007) and for the NO production triggered by NMDAR activation by modulating the phosphorylation state of nNOS (Park et al., 2008a; Iadecola, 2017). Our

observation that the beneficial effect of tPA on functional hyperemia is prevented by the LRP1 inhibitor RAP would support this hypothesis. However, RAP also inhibits lipoprotein receptors activated by ligands other than tPA, which can also impact NMDAR signaling (Herz, 2001; Samson and Medcalf, 2006). Therefore, the role of LRP1 in the relationship between tPA and NMDAR signaling needs more exploration. Furthermore, although PAI-1 inhibition ameliorates neurovascular and cognitive dysfunction in aged tg2576 mice, the role of the tPA–NMDAR–NO pathway needs to be explored further at this age.

Our data that tPA activity is reduced and PAI-1 activity is increased in tg2576 mice are consistent with similar findings in AD and mouse models (Tucker et al., 2000; Melchor et al., 2003; Cacquevel et al., 2007; Jacobsen et al., 2008; Hanzel et al., 2014; Oh et al., 2014). Increases in PAI-1 expression and activity have also been described in several cardiovascular diseases (Rosenberg and Aird, 1999; Jung et al., 2018; Yu et al., 2019). In these conditions, the upregulation has been attributed to oxidative stress, which promotes PAI-1 expression and/or activation (Nicholl et al., 2006; Collins-Underwood et al., 2008; Zhao et al., 2009; Sangle et al., 2010; Ko et al., 2015), or a loss of NO, which has been shown to suppress PAI-1 activity (Katoh et al., 2000; Kaikita et al., 2001). The mechanisms by which Aβ upregulates PAI-1 activity remain unclear and, although Aβ-derived ROS could play a role, supportive evidence is lacking. Irrespective of how amyloid pathology increases PAI-1 activity, previous studies have shown that reconstituting tPA activity reduces amyloid plaques and ameliorates cognitive function in mouse models (Melchor et al., 2003; Jacobsen et al., 2008; Oh et al., 2014). These effects were attributed to the ability of the tPA to promote the breakdown of Aβ through a direct proteolytic effect of plasmin or by upregulating Aβ degrading enzymes (Miners et al., 2008). In agreement with these studies, we also found that the rescue of tPA activity by inhibition of PAI-1 for 4 weeks in aged tg2576 mice improves neurovascular coupling and cognition. However, these improvements were not associated with a reduction in A$\beta_{1–42}$ and amyloid plaques, but with a reduction in A$\beta_{1–40}$ and CAA. This outcome is anticipated based on the fact that A$\beta_{1–40}$ accumulates predominantly in cerebral blood vessels and A$\beta_{1–42}$ in plaques, and is consistent with the finding that deletion of the scavenger receptor CD36 ameliorates CAA and reduces A$\beta_{1–40}$ but not amyloid plaques and Aβ_{1-42} (Park et al., 2008b, 2013). These observations raise the possibility that re-establishing neurovascular function with tPA may also promote A$\beta_{1–40}$ clearance by cerebral blood vessels, one of the main pathways for Aβ disposal (Iadecola, 2013, 2017; Tarasoff-Conway et al., 2016). Considering that tPA did not improve endothelium-dependent relaxation, rescue of neurovascular coupling could be sufficient to ameliorate cognitive function and CAA. However, concomitant beneficial effects of tPA on Aβ degradation and synaptic plasticity cannot be excluded and could also play a role.

Our data implicate a loss of tPA activity in the mechanisms of CAA, a major cause of cortical hemorrhages in the elderly and a key component of AD pathology (Greenberg et al., 2020). The finding that rescuing tPA activity reduces vascular amyloid accumulation suggests a potential beneficial role in CAA. Preservation of tPA activity could also be beneficial in amyloid-related imaging abnormalities, an adverse effect of anti-Aβ immunotherapy (Sperling, 2011) characterized by perivascular inflammation, microhemorrhages, and edema attributed to the vascular effects of Aβ released from amyloid plaques (Boche et al., 2010; Sakai et al., 2014). However, increasing tPA activity in CAA raises the concern that the resulting increase of fibrinolysis may cause cerebral hemorrhage, especially in ApoE2 carriers who are more prone to hemorrhages in CAA and in ApoE4 carrier in whom the blood–brain barrier is compromised (Greenberg et al., 2020; Montagne et al., 2020). On the other hand, treatment with anticoagulants has been advocated and shown to be effective in animal models by reducing fibrin (Cortes-Canteli et al., 2010, 2019). Therefore, modulation of PAI-1-tPA for therapy may be promising and requires further scrutiny.

In conclusion, we have demonstrated that reduced tPA activity is responsible specifically for the attenuation in neurovascular coupling, but not for the endothelial dysfunction, in tg2576 mice or in WT mice treated with Aβ. The mechanisms of effect involve uncoupling NMDAR activity from NO production from nNOS, possibly by engaging LRP1. The attenuation in tPA is secondary to upregulation of PAI-1 activity, and inhibition of PAI-1 increases tPA and leads to a full rescue of the neurovascular dysfunction and cognitive impairment in aged tg2576 mice, effects associated with a reduction in CAA, but not amyloid plaques. The data unveil a previously unappreciated diversity in the effects of Aβ on the cerebral vasculature and a specific involvement of tPA in the pathobiology of CAA, with potential therapeutic implications.

References

Anfray A, Drieu A, Hingot V, Hommet Y, Yetim M, Rubio M, Deffieux T, Tanter M, Orset C, Vivien D (2020) Circulating tPA contributes to neurovascular coupling by a mechanism involving the endothelial NMDA receptors. J Cereb Blood Flow Metab 40:2038–2054.

Baranes D, Lederfein D, Huang YY, Chen M, Bailey CH, Kandel ER (1998) Tissue plasminogen activator contributes to the late phase of LTP and to synaptic growth in the hippocampal mossy fiber pathway. Neuron 21:813–825.

Benchenane K, López-Atalaya JP, Fernández-Monreal M, Touzani O, Vivien D (2004) Equivocal roles of tissue-type plasminogen activator in stroke-induced injury. Trends Neurosci 27:155–160.

Boche D, Denham N, Holmes C, Nicoll JA (2010) Neuropathology after active Abeta42 immunotherapy: implications for Alzheimer's disease pathogenesis. Acta Neuropathol 120:369–384.

Cacquevel M, Launay S, Castel H, Benchenane K, Chéenne S, Buée L, Moons L, Delacourte A, Carmeliet P, Vivien D (2007) Ageing and amyloid-beta peptide deposition contribute to an impaired brain tissue plasminogen activator activity by different mechanisms. Neurobiol Dis 27:164–173.

Capone C, Anrather J, Milner TA, Iadecola C (2009) Estrous cycle-dependent neurovascular dysfunction induced by angiotensin II in the mouse neocortex. Hypertension 54:302–307.

Capone C, Faraco G, Park L, Cao X, Davisson RL, Iadecola C (2011) The cerebrovascular dysfunction induced by slow pressor doses of angiotensin II precedes the development of hypertension. Am J Physiol Heart Circ Physiol 300:H397–H407.

Carmeliet P, Kieckens L, Schoonjans L, Ream B, van Nuffelen A, Prendergast G, Cole M, Bronson R, Collen D, Mulligan RC (1993) Plasminogen activator inhibitor-1 gene-deficient mice. I. Generation by homologous recombination and characterization. J Clin Invest 92:2746–2755.

Carmeliet P, Schoonjans L, Kieckens L, Ream B, Degen J, Bronson R, De Vos R, van den Oord JJ, Collen D, Mulligan RC (1994) Physiological consequences of loss of plasminogen activator gene function in mice. Nature 368:419–424.

Chandler HL, Wise RG, Murphy K, Tansey KE, Linden DEJ, Lancaster TM (2019) Polygenic impact of common genetic risk loci for Alzheimer's disease on cerebral blood flow in young individuals. Sci Rep 9:467.

Coleman CG, Wang G, Park L, Anrather J, Delagrammatikas GJ, Chan J, Zhou J, Iadecola C, Pickel VM (2010) Chronic intermittent hypoxia induces NMDA receptor-dependent plasticity and suppresses nitric oxide signaling in the mouse hypothalamic paraventricular nucleus. J Neurosci 30:12103–12112.

Collins-Underwood JR, Zhao W, Sharpe JG, Robbins ME (2008) NADPH oxidase mediates radiation-induced oxidative stress in rat brain microvascular endothelial cells. Free Radic Biol Med 45:929–938.

Cortes-Canteli M, Iadecola C (2020) Alzheimer's disease and vascular aging: JACC focus seminar. J Am Coll Cardiol 75:942–951.

Cortes-Canteli M, Paul J, Norris EH, Bronstein R, Ahn HJ, Zamolodchikov D, Bhuvanendran S, Fenz KM, Strickland S (2010) Fibrinogen and beta-amyloid association alters thrombosis and fibrinolysis: a possible contributing factor to Alzheimer's disease. Neuron 66:695–709.

Cortes-Canteli M, Kruyer A, Fernandez-Nueda I, Marcos-Diaz A, Ceron C, Richards AT, Jno-Charles OC, Rodriguez I, Callejas S, Norris EH, Sanchez-Gonzalez J, Ruiz-Cabello J, Ibanez B, Strickland S, Fuster V (2019) Long-term dabigatran treatment delays Alzheimer's disease pathogenesis in the TgCRND8 mouse model. J Am Coll Cardiol 74:1910–1923.

Crandall DL, Quinet EM, El Ayachi S, Hreha AL, Leik CE, Savio DA, Juhan-Vague I, Alessi MC (2006) Modulation of adipose tissue development by pharmacological inhibition of PAI-1. Arterioscler Thromb Vasc Biol 26:2209–2215.

Deane R, Wu Z, Sagare A, Davis J, Du Yan S, Hamm K, Xu F, Parisi M, LaRue B, Hu HW, Spijkers P, Guo H, Song X, Lenting PJ, Van Nostrand WE, Zlokovic BV (2004) LRP/amyloid beta-peptide interaction mediates differential brain efflux of Abeta isoforms. Neuron 43:333–344.

Dellu F, Contarino A, Simon H, Koob GF, Gold LH (2000) Genetic differences in response to novelty and spatial memory using a two-trial recognition task in mice. Neurobiol Learn Mem 73:31–48.

Diaz A, Jeanneret V, Merino P, McCann P, Yepes M (2019) Tissue-type plasminogen activator regulates p35-mediated Cdk5 activation in the postsynaptic terminal. J Cell Sci 132:jcs224196.

Elokdah H, Abou-Gharbia M, Hennan JK, McFarlane G, Mugford CP, Krishnamurthy G, Crandall DL (2004) Tiplaxtinin, a novel, orally efficacious inhibitor of plasminogen activator inhibitor-1: design, synthesis, and preclinical characterization. J Med Chem 47:3491–3494.

Faraco G, Park L, Anrather J, Iadecola C (2017) Brain perivascular macrophages: characterization and functional roles in health and disease. J Mol Med (Berl) 95:1143–1152.

Faraco G, Brea D, Garcia-Bonilla L, Wang G, Racchumi G, Chang H, Buendia I, Santisteban MM, Segarra SG, Koizumi K, Sugiyama Y, Murphy M, Voss H, Anrather J, Iadecola C (2018) Dietary salt promotes neurovascular and cognitive dysfunction through a gut-initiated TH17 response. Nat Neurosci 21:240–249.

Franklin K, Paxinos G (1997) The mouse brain in stereotaxic coordinates. San Diego: Academic.

Girouard H, Lessard A, Capone C, Milner TA, Iadecola C (2008) The neurovascular dysfunction induced by angiotensin II in the mouse neocortex is sexually dimorphic. Am J Physiol Heart Circ Physiol 294:H156–H163.

Gotthardt M, Trommsdorff M, Nevitt MF, Shelton J, Richardson JA, Stockinger W, Nimpf J, Herz J (2000) Interactions of the low density lipoprotein receptor gene family with cytosolic adaptor and scaffold proteins suggest diverse biological functions in cellular communication and signal transduction. J Biol Chem 275:25616–25624.

Greenberg SM, Bacskai BJ, Hernandez-Guillamon M, Pruzin J, Sperling R, van Veluw SJ (2020) Cerebral amyloid angiopathy and Alzheimer disease–one peptide, two pathways. Nat Rev Neurol 16:30–42.

Griemert EV, Schwarzmaier SM, Hummel R, Gölz C, Yang D, Neuhaus W, Burek M, Förster CY, Petkovic I, Trabold R, Plesnila N, Engelhard K, Schäfer MK, Thal SC (2019) Plasminogen activator inhibitor-1 augments damage by impairing fibrinolysis after traumatic brain injury. Ann Neurol 85:667–680.

Hanzel CE, Iulita MF, Eyjolfsdottir H, Hjorth E, Schultzberg M, Eriksdotter M, Cuello AC (2014) Analysis of matrix metallo-proteases and the plasminogen system in mild cognitive impairment and Alzheimer's disease cerebrospinal fluid. J Alzheimers Dis 40:667–678.

Hennan JK, Morgan GA, Swillo RE, Antrilli TM, Mugford C, Vlasuk GP, Gardell SJ, Crandall DL (2008) Effect of tiplaxtinin (PAI-039), an orally bioavailable PAI-1 antagonist, in a rat model of thrombosis. J Thromb Haemost 6:1558–1564.

Herz J (2001) The LDL receptor gene family: (un)expected signal transducers in the brain. Neuron 29:571–581.

Hsiao K, Chapman P, Nilsen S, Eckman C, Harigaya Y, Younkin S, Yang F, Cole G (1996) Correlative memory deficits, Abeta elevation, and amyloid plaques in transgenic mice. Science 274:99–102.

Iadecola C (1992) Nitric oxide participates in the cerebrovasodilation elicited from cerebellar fastigial nucleus. Am J Physiol 263:R1156–R1161.

Iadecola C (2013) The pathobiology of vascular dementia. Neuron 80:844–866.

Iadecola C (2017) The neurovascular unit coming of age: a journey through neurovascular coupling in health and disease. Neuron 96:17–42.

Iadecola C, Zhang F, Niwa K, Eckman C, Turner SK, Fischer E, Younkin S, Borchelt DR, Hsiao KK, Carlson GA (1999) SOD1 rescues cerebral endothelial dysfunction in mice overexpressing amyloid precursor protein. Nat Neurosci 2:157–161.

Iturria-Medina Y, Sotero RC, Toussaint PJ, Mateos-Pérez JM, Evans AC (2016) Early role of vascular dysregulation on late-onset Alzheimer's disease based on multifactorial data-driven analysis. Nat Commun 7:11934.

Jackman K, Kahles T, Lane D, Garcia-Bonilla L, Abe T, Capone C, Hochrainer K, Voss H, Zhou P, Ding A, Anrather J, Iadecola C (2013) Progranulin deficiency promotes post-ischemic blood-brain barrier disruption. J Neurosci 33:19579–19589.

Jacobsen JS, Comery TA, Martone RL, Elokdah H, Crandall DL, Oganesian A, Aschmies S, Kirksey Y, Gonzales C, Xu J, Zhou H, Atchison K, Wagner E, Zaleska MM, Das I, Arias RL, Bard J, Riddell D, Gardell SJ, Abou-Gharbia M, et al (2008) Enhanced clearance of Abeta in brain by sustaining the plasmin proteolysis cascade. Proc Natl Acad Sci U S A 105:8754–8759.

Jung RG, Motazedian P, Ramirez FD, Simard T, Di Santo P, Visintini S, Faraz MA, Labinaz A, Jung Y, Hibbert B (2018) Association between plasminogen activator inhibitor-1 and cardiovascular events: a systematic review and meta-analysis. Thromb J 16:12.

Kaikita K, Fogo AB, Ma L, Schoenhard JA, Brown NJ, Vaughan DE (2001) Plasminogen activator inhibitor-1 deficiency prevents hypertension and vascular fibrosis in response to long-term nitric oxide synthase inhibition. Circulation 104:839–844.

Katoh M, Egashira K, Mitsui T, Chishima S, Takeshita A, Narita H (2000) Angiotensin-converting enzyme inhibitor prevents plasminogen activator inhibitor-1 expression in a rat model with cardiovascular remodeling induced by chronic inhibition of nitric oxide synthesis. J Mol Cell Cardiol 32:73–83.

Ko HM, Lee SH, Kim KC, Joo SH, Choi WS, Shin CY (2015) The role of TLR4 and Fyn interaction on lipopolysaccharide-stimulated PAI-1 expression in astrocytes. Mol Neurobiol 52:8–25.

Koizumi K, Hattori Y, Ahn SJ, Buendia I, Ciacciarelli A, Uekawa K, Wang G, Hiller A, Zhao L, Voss HU, Paul SM, Schaffer C, Park L, Iadecola C (2018) Apoε4 disrupts neurovascular regulation and undermines white matter integrity and cognitive function. Nat Commun 9:3816.

Leger M, Quiedeville A, Bouet V, Haelewyn B, Boulouard M, Schumann-Bard P, Freret T (2013) Object recognition test in mice. Nat Protoc 8:2531–2537.

Long JM, Holtzman DM (2019) Alzheimer disease: an update on pathobiology and treatment strategies. Cell 179:312–339.

Mantuano E, Lam MS, Gonias SL (2013) LRP1 assembles unique co-receptor systems to initiate cell signaling in response to tissue-type plasminogen activator and myelin-associated glycoprotein. J Biol Chem 288:34009–34018.

Martin AM, Kuhlmann C, Trossbach S, Jaeger S, Waldron E, Roebroek A, Luhmann HJ, Laatsch A, Weggen S, Lessmann V, Pietrzik CU (2008) The functional role of the second NPXY motif of the LRP1 beta-chain in tissue-type plasminogen activator-mediated activation of N-methyl-D-aspartate receptors. J Biol Chem 283:12004–12013.

May P, Rohlmann A, Bock HH, Zurhove K, Marth JD, Schomburg ED, Noebels JL, Beffert U, Sweatt JD, Weeber EJ, Herz J (2004) Neuronal LRP1 functionally associates with postsynaptic proteins and is required for normal motor function in mice. Mol Cell Biol 24:8872–8883.

Melchor JP, Pawlak R, Strickland S (2003) The tissue plasminogen activator-plasminogen proteolytic cascade accelerates amyloid-beta (Abeta) degradation and inhibits Abeta-induced neurodegeneration. J Neurosci 23:8867–8871.

Mentis MJ, Alexander GE, Krasuski J, Pietrini P, Furey ML, Schapiro MB, Rapoport SI (1998) Increasing required neural response to expose abnormal brain function in mild versus moderate or severe Alzheimer's disease: PET study using parametric visual stimulation. Am J Psychiatry 155:785–794.

Miners JS, Baig S, Palmer J, Palmer LE, Kehoe PG, Love S (2008) Abeta-degrading enzymes in Alzheimer's disease. Brain Pathol 18:240–252.

Montagne A, Nation DA, Sagare AP, Barisano G, Sweeney MD, Chakhoyan A, Pachicano M, Joe E, Nelson AR, D'Orazio LM, Buennagel DP, Harrington MG, Benzinger TLS, Fagan AM, Ringman JM, Schneider LS, Morris JC, Reiman EM, Caselli RJ, Chui HC, et al. (2020) *APOE4* leads to blood–brain barrier dysfunction predicting cognitive decline. Nature 581:71–76.

Nakajima C, Kulik A, Frotscher M, Herz J, Schäfer M, Bock HH, May P (2013) Low density lipoprotein receptor-related protein 1 (LRP1) modulates N-methyl-D-aspartate (NMDA) receptor-dependent intracellular signaling and NMDA-induced regulation of postsynaptic protein complexes. J Biol Chem 288:21909–21923.

Nicholl SM, Roztocil E, Davies MG (2006) Plasminogen activator system and vascular disease. Curr Vasc Pharmacol 4:101–116.

Nicole O, Docagne F, Ali C, Margaill I, Carmeliet P, MacKenzie ET, Vivien D, Buisson A (2001) The proteolytic activity of tissue-plasminogen activator enhances NMDA receptor-mediated signaling. Nat Med 7:59–64.

Niwa K, Carlson GA, Iadecola C (2000a) Exogenous A beta1-40 reproduces cerebrovascular alterations resulting from amyloid precursor protein overexpression in mice. J Cereb Blood Flow Metab 20:1659–1668.

Niwa K, Araki E, Morham SG, Ross ME, Iadecola C (2000b) Cyclooxygenase-2 contributes to functional hyperemia in whisker-barrel cortex. J Neurosci 20:763–770.

Niwa K, Younkin L, Ebeling C, Turner SK, Westaway D, Younkin S, Ashe KH, Carlson GA, Iadecola C (2000c) Abeta 1-40-related reduction in functional hyperemia in mouse neocortex during somatosensory activation. Proc Natl Acad Sci U S A 97:9735–9740.

Niwa K, Porter VA, Kazama K, Cornfield D, Carlson GA, Iadecola C (2001) Aβ-peptides enhance vasoconstriction in cerebral circulation. Am J Physiol Heart Circ Physiol 281:H2417–H2424.

Niwa K, Kazama K, Younkin SG, Carlson GA, Iadecola C (2002a) Alterations in cerebral blood flow and glucose utilization in mice overexpressing the amyloid precursor protein. Neurobiol Dis 9:61–68.

Niwa K, Kazama K, Younkin L, Younkin SG, Carlson GA, Iadecola C (2002b) Cerebrovascular autoregulation is profoundly impaired in mice overexpressing amyloid precursor protein. Am J Physiol Heart Circ Physiol 283:H315–H323.

Norris EH, Strickland S (2007) Modulation of NR2B-regulated contextual fear in the hippocampus by the tissue plasminogen activator system. Proc Natl Acad Sci USA U S A 104:13473–13478.

Nortley R, Korte N, Izquierdo P, Hirunpattarasilp C, Mishra A, Jaunmuktane Z, Kyrargyri V, Pfeiffer T, Khennouf L, Madry C, Gong H, Richard-Loendt A, Huang W, Saito T, Saido TC, Brandner S, Sethi H, Attwell D (2019) Amyloid β oligomers constrict human capillaries in Alzheimer's disease via signaling to pericytes. Science 365:eaav9518.

Oh SB, Byun CJ, Yun JH, Jo DG, Carmeliet P, Koh JY, Lee JY (2014) Tissue plasminogen activator arrests Alzheimer's disease pathogenesis. Neurobiol Aging 35:511–519.

Park L, Anrather J, Forster C, Kazama K, Carlson GA, Iadecola C (2004) Abeta-induced vascular oxidative stress and attenuation of functional hyperemia in mouse somatosensory cortex. J Cereb Blood Flow Metab 24:334–342.

Park L, Anrather J, Zhou P, Frys K, Pitstick R, Younkin S, Carlson GA, Iadecola C (2005) NADPH-oxidase-derived reactive oxygen species mediate the cerebrovascular dysfunction induced by the amyloid β peptide. J Neurosci 25:1769–1777.

Park L, Gallo EF, Anrather J, Wang G, Norris EH, Paul J, Strickland S, Iadecola C (2008a) Key role of tissue plasminogen activator in neurovascular coupling. Proc Natl Acad Sci U S A 105:1073–1078.

Park L, Zhou P, Pitstick R, Capone C, Anrather J, Norris EH, Younkin L, Younkin S, Carlson G, McEwen BS, Iadecola C (2008b) Nox2-derived radicals contribute to neurovascular and behavioral dysfunction in mice overexpressing the amyloid precursor protein. Proc Natl Acad Sci U S A 105:1347–1352.

Park L, Wang G, Zhou P, Zhou J, Pitstick R, Previti ML, Younkin L, Younkin SG, Van Nostrand WE, Cho S, Anrather J, Carlson GA, Iadecola C (2011) Scavenger receptor CD36 is essential for the cerebrovascular oxidative stress and neurovascular dysfunction induced by amyloid-beta. Proc Natl Acad Sci U S A 108:5063–5068.

Park L, Zhou J, Zhou P, Pistick R, El Jamal S, Younkin L, Pierce J, Arreguin A, Anrather J, Younkin SG, Carlson GA, McEwen BS, Iadecola C (2013) Innate immunity receptor CD36 promotes cerebral amyloid angiopathy. Proc Natl Acad Sci U S A 110:3089–3094.

Park L, Wang G, Moore J, Girouard H, Zhou P, Anrather J, Iadecola C (2014) The key role of transient receptor potential melastatin-2 channels in amyloid-β-induced neurovascular dysfunction. Nat Commun 5:5318.

Park L, Uekawa K, Garcia-Bonilla L, Koizumi K, Murphy M, Pistik R, Younkin L, Younkin S, Zhou P, Carlson G, Anrather J, Iadecola C (2017) Brain Perivascular Macrophages Initiate the Neurovascular Dysfunction of Alzheimer Aβ Peptides. Circ Res 121:258–269.

Park L, Hochrainer K, Hattori Y, Ahn SJ, Anfray A, Wang G, Uekawa K, Seo J, Palfini V, Blanco I, Acosta D, Eliezer D, Zhou P, Anrather J, Iadecola C (2020) Tau induces PSD95–neuronal NOS uncoupling and neurovascular dysfunction independent of neurodegeneration. Nat Neurosci 23:1079–1089.

Percie du Sert N, Hurst V, Ahluwalia A, Alam S, Avey MT, Baker M, Browne WJ, Clark A, Cuthill IC, Dirnagl U, Emerson M, Garner P, Holgate ST, Howells DW, Karp NA, Lazic SE, Lidster K, MacCallum CJ, Macleod M, Pearl EJ, et al. (2020) The ARRIVE guidelines 2.0: updated guidelines for reporting animal research. PLoS Biol 18:e3000410.

Rosenberg RD, Aird WC (1999) Vascular-bed–specific hemostasis and hypercoagulable states. N Engl J Med 340:1555–1564.

Sakai K, Boche D, Carare R, Johnston D, Holmes C, Love S, Nicoll JA (2014) Aβ immunotherapy for Alzheimer's disease: effects on apoE and cerebral vasculopathy. Acta Neuropathol 128:777–789.

Samson AL, Medcalf RL (2006) Tissue-type plasminogen activator: a multifaceted modulator of neurotransmission and synaptic plasticity. Neuron 50:673–678.

Samson AL, Nevin ST, Croucher D, Niego B, Daniel PB, Weiss TW, Moreno E, Monard D, Lawrence DA, Medcalf RL (2008) Tissue-type plasminogen activator requires a co-receptor to enhance NMDA receptor function. J Neurochem 107:1091–1101.

Sangle GV, Zhao R, Mizuno TM, Shen GX (2010) Involvement of RAGE, NADPH oxidase, and Ras/Raf-1 pathway in glycated LDL-induced expression of heat shock factor-1 and plasminogen activator inhibitor-1 in vascular endothelial cells. Endocrinology 151:4455–4466.

Shibata M, Yamada S, Kumar SR, Calero M, Bading J, Frangione B, Holtzman DM, Miller CA, Strickland DK, Ghiso J, Zlokovic BV (2000) Clearance of Alzheimer's amyloid-$\beta_{(1\text{-}40)}$ peptide from brain by LDL receptor-related protein-1 at the blood-brain barrier. J Clin Invest 106:1489–1499.

Smith EE, Vijayappa M, Lima F, Delgado P, Wendell L, Rosand J, Greenberg SM (2008) Impaired visual evoked flow velocity response in cerebral amyloid angiopathy. Neurology 71:1424–1430.

Spellman T, Rigotti M, Ahmari SE, Fusi S, Gogos JA, Gordon JA (2015) Hippocampal-prefrontal input supports spatial encoding in working memory. Nature 522:309–314.

Sperling RA (2011) Toward defining the preclinical stages of Alzheimer's disease: recommendations from the National Institute on Aging-Alzheimer's Association workgroups on diagnostic guidelines for Alzheimer's disease. Alzheimers Dement 7:280–292.

Sweeney MD, Kisler K, Montagne A, Toga AW, Zlokovic BV (2018) The role of brain vasculature in neurodegenerative disorders. Nat Neurosci 21:1318–1331.

Tarasoff-Conway JM, Carare RO, Osorio RS, Glodzik L, Butler T, Fieremans E, Axel L, Rusinek H, Nicholson C, Zlokovic BV, Frangione B, Blennow K, Ménard J, Zetterberg H, Wisniewski T, de Leon MJ (2016) Clearance systems in the brain–implications for Alzheimer diseaser. Nat Rev Neurol 12:248.

Thomas T, Thomas G, McLendon C, Sutton T, Mullan M (1996) beta-Amyloid-mediated vasoactivity and vascular endothelial damage. Nature 380:168–171.

Tong XK, Lecrux C, Rosa-Neto P, Hamel E (2012) Age-dependent rescue by simvastatin of Alzheimer's disease cerebrovascular and memory deficits. J Neurosci 32:4705–4715.

Tucker HM, Kihiko M, Caldwell JN, Wright S, Kawarabayashi T, Price D, Walker D, Scheff S, McGillis JP, Rydel RE, Estus S (2000) The plasmin system is induced by and degrades amyloid-beta aggregates. J Neurosci 20:3937–3946.

Uekawa K, Koizumi K, Hwang J, Brunier N, Hattori Y, Zhou P, Park L (2016) Obligatory role of EP1 receptors in the increase in cerebral blood flow produced by hypercapnia in the mice. PLoS One 11:e0163329.

Vorhees CV, Williams MT (2014) Assessing spatial learning and memory in rodents. ILAR J 55:310–332.

Wang G, Coleman CG, Chan J, Faraco G, Marques-Lopes J, Milner TA, Guruju MR, Anrather J, Davisson RL, Iadecola C, Pickel VM (2013) Angiotensin II slow-pressor hypertension enhances NMDA currents and NOX2-dependent superoxide production in hypothalamic paraventricular neurons. Am J Physiol Regul Integr Comp Physiol 304: R1096–R1106.

Wenk GL (2004) Assessment of spatial memory using the radial arm maze and Morris water maze. Curr Protoc Neurosci Chapter 8:Unit 8.5A.

Yang G, Chen G, Ebner TJ, Iadecola C (1999) Nitric oxide is the predominant mediator of cerebellar hyperemia during somatosensory activation in rats. Am J Physiol 277:R1760–R1770.

Yu P, Venkat P, Chopp M, Zacharek A, Shen Y, Liang L, Landschoot-Ward J, Liu Z, Jiang R, Chen J (2019) Deficiency of tPA exacerbates white matter damage, neuroinflammation, glymphatic dysfunction and cognitive dysfunction in aging mice. Aging Dis 10:770–783.

Zhao L, Gottesdiener AJ, Parmar M, Li M, Kaminsky SM, Chiuchiolo MJ, Sondhi D, Sullivan PM, Holtzman DM, Crystal RG, Paul SM (2016) Intracerebral adeno-associated virus gene delivery of apolipoprotein E2 markedly reduces brain amyloid pathology in Alzheimer's disease mouse models. Neurobiol Aging 44:159–172.

Zhao R, Ma X, Xie X, Shen GX (2009) Involvement of NADPH oxidase in oxidized LDL-induced upregulation of heat shock factor-1 and plasminogen activator inhibitor-1 in vascular endothelial cells. Am J Physiol Endocrinol Metab 297:E104–E111.